Waste Heat Recovery in Brake Pad using a Thermoelectric Generator

Experimental Study

10th semester student project, TEPE 2012

Appendix Report

Loïc Courant

Supervisor:

Lasse Aistrup Rosendahl

Submitted:

31.05.2012

Group:

TEPE4 - 1007

Alborg University

Department of Energy Technology

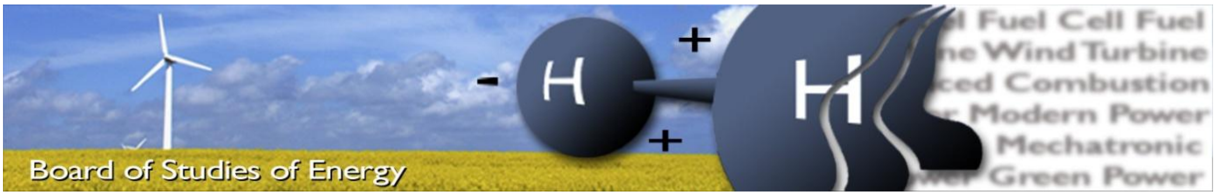

Title: **Waste heat recovery in brake pad using a thermoelectric generator**

Experimental study

Semester: 10th

Semester theme:

Project period: 01/02/2012 to 31/05/2012

ECTS: 30

Supervisor: Lasse Aistrup Rosendahl

Project group: TEPE4- 1007

____

Loïc COURANT

Copies: 2

Pages, total: 73

Appendix: 13

Supplements: CD

SYNOPSIS:

Slowing down the increase of the energy consumption's is one of the main challenge of this decade.

Transporting is one of the biggest energy consuming sector. So, to increase the efficiency of our vehicles, energy harvesting has become more and more widespread in the transports' study field.

According to literature, during breaking, an heavy vehicle can waste from 400 to 3000 [kW] mostly converted into heat. That suggest that a large energy recuperation might be possible in this area.

However, finding an energy harvesting technology at a scale of our braking system may seem problematic, since most of them as scalability problems.

Thermoelectric generator (TEG), might match this problematic.

After carring out several experiments to understand and analyse the heat behavior and the energy recovery in different brake pads, we finaly find out that our concept of using a TEG to to recover waste energy is not adaptable to a medium range car.

But making some improvements and using it in bigger vehicles could still be an interesting field of investigation.

By signing this document, each member of the group confirms that all group members have participated in the project work, and thereby all members are collectively liable for the contents of the report. Furthermore, all group members confirm that the report does not include plagiarism.

Contents

1 Introduction

With the increasing price of oil, the growing concern on energy conservation and the introduction of new legislations on greenhouse gas emissions, the development of energy-efficient technologies has taken on an accelerated pace.

If a majority of industries have managed to reduce their energy consumption for 30 years, the worldwide transport consumption is still increasing. This trend is mainly explained by the increasing amount of vehicles in circulation. However, current vehicles still use low efficiency technologies and many improvements are possible in this sector. **[Syrota, 2008]**

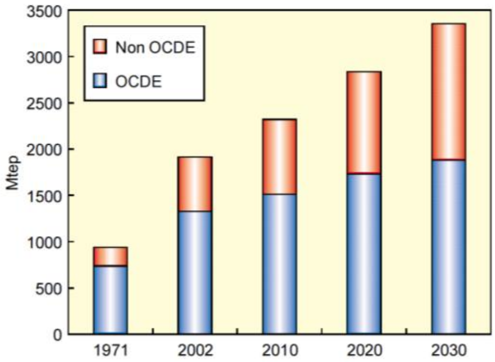

figure 1.1: Evolution of the transport energy consumption in Mtep (Mtone petrol equivalent) since 1971, with a projection to 2030

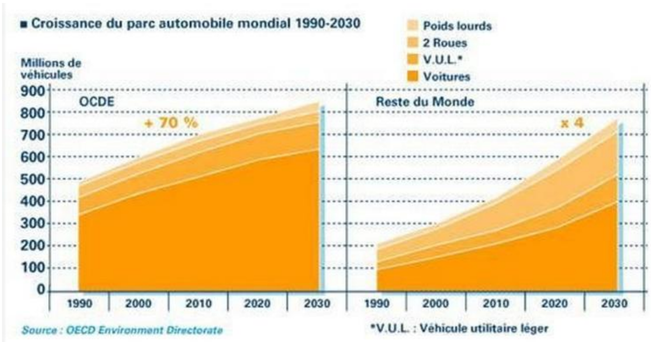

figure 1.2: Evolution of the amount of vehicles in circulation in the OCDE countries and in the rest of the world.

With this two figures we can see that the energy consumption is following the number of vehicles in circulation. The main concern is the increased consumption that is going to exceed all reasonable limits. Finding solutions to avoid this problem is not only essential but vital for the future of our society.**[Plouchard, 2004]**

According to **[Congress, 2011]**, a lot of improvements have already been done, especially in terms of engine efficiency and heat recovery. The average fuel consumption of our vehicles has been steadily decreasing since the last seven years. However we still have much to do to reverse the increase in global road transport consumption.

One of the main feature of road transport is the repetition of acceleration and deceleration phases. We know that during the braking, most of the energy is dissipated as heat. Indeed on most vehicles braking is done by the friction of two brake pads on a disc which increase a lot the temperature of those elements. The brake energy depends mostly on two factors which are the speed and weight of the vehicles.

The energy dissipated during braking is equal to the loss of kinetic energy, so with a simple calculation, we can find that for a 1000kg car with a speed of 20m/s, the braking energy loss to bring it to 0m/s will be around 200kJ. That correspond to the energy dissipated by the combustion of 5cL of diesel.

The most interesting situation might be the braking to maintain a constant speed during a downhill. The energy dissipated into heat during this constant breaking is so important, that it can even be dangerous for the breaking system.

Last case of energy wasted during braking is the railroad transport especially metros and tramways. Indeed this two common transports are used to accelerate and brake a lot. They are dissipating a huge amount of energy which is often wasted and might be recovered.

These examples show how the brake represents a significant loss of energy and therefore is an interesting area of study for energy harvesting.

In this regard, some braking energy recovery systems have already been developed. We can for example talk about the regenerative braking system used on electrics and hybrid cars. This system uses the reversibility of the electric motor to generate electricity while slowing down the vehicle. The biggest disadvantage of this system is his weight. So on, it is only easily adaptable to vehicles already using an electric motor. Indeed installation on thermal vehicles would increase its weight and its energy consumption. The other main system used to recover the energy wasted during braking is the flywheels. Flywheel energy storage works by accelerating a rotor to a very high speed and maintaining the energy as rotational energy. Compared with the others ways to store energy, flywheels have a large maximum power output, but it is an large and heavy system, more adaptable on train than on road vehicles **[Techniques de l'ingénieur, 2011]**.

Another way to recover the energy wasted during braking might be using a Thermoelectric Generator. TEGs are made from thermoelectric modules that employ three thermoelectric effects known as the Peltier, Seebeck and Thomson effects. The electricity generation is allowed by the Seebeck effect. A TEG consists of pairs of semiconductor materials forming thermocouples. These thermocouples are then connected electrically. They are then sandwiched between two ceramic wafers. When a temperature gradient is applied between this two wafers, this device then generates electricity **[Stockohlm,2002]**.

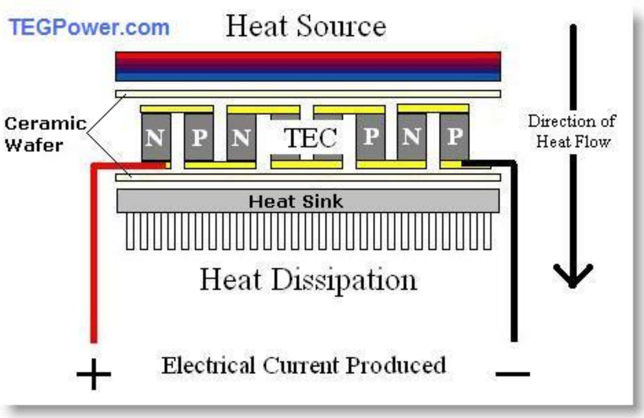

figure 1.3: mapping of the composition of a TEG
[TEGPower.com]

Even if Thomas Johann Seebeck discovered the thermoelectric effect in 1821, the first real use of a thermoelectric generator was in 1977 with the launch of the spacecraft "voyager" by the NASA. Since then the low efficiency of TEG limits their use to systems in which reliability and durability are more important than performance.

However, thanks to new researches on the thermoelectric elements, the performance of TEG have been effectively improved. This has arisen the interest of many new market segments as the one of transport. TEG have been recently used to recover energy from exhaust gas or from the heat lost in the car radiator. But thanks to their characteristics TEG might be a really interesting way to recover energy from braking systems. Indeed thermoelectric generator are cheap, small, reliable, have no moving parts or fluid and do not add extra weight **[Rosendahl, 2011]**, they could therefore be quite easily integrated to brake pads as shown in fig 1.4**.**

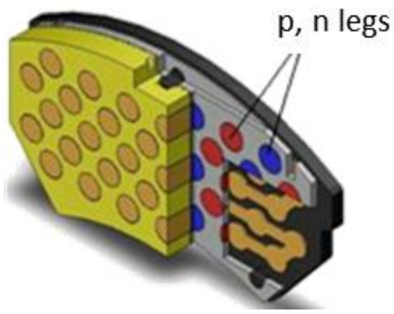

figure 1.4: A CAD of the incorporation of thermoelectric elements in a brake

As explained before, using a thermoelectric generator as a regenerative braking system is an untested application area for now. This is why Alpcon and Aalborg University have decided to investigate this new application and applied for a patent to protect the design. The purpose of this study is to perform a validation of the modeling concept and carrying out experiments to study the potential for this application.

The project started in the second half of 2011, with a team consisting of Rene Haller Schultz, Troels Bartholin Bertelsen and Thomas Helmer Pederson. They have studied the theoretical behavior of the system and perform a numerical modeling of it. The study we will carry out will be focus on achieving a series of experiments and analysis to confirm or refute the findings obtained by numerical modeling. The purpose of this experiment will be to obtain the heat generation measurement, the different temperature profiles following the three axis of the pad and the real amount of energy we can get from the TEG under different conditions. All these experiments will be carried out in different conditions to understand as much as possible the comportment of the system.

Analyzing all these experiments will help us to conclude on the viability of using TEG as an energy harvesting system during the deceleration of an heavy vehicle.

2 Thesis statement

Slowing down the increase of the energy consumption's is one of the main challenge of this decade. In response we will need to increase the efficiency of our processes.

Transporting is one of the biggest energy consuming sector. So, to increase the efficiency of our vehicles, energy harvesting has become more and more widespread in the transports' study field.

According to literature, during breaking, an heavy vehicle can waste from 400 to 3000 [kW] mostly converted into heat. That suggest that a large energy recuperation might be possible in this area.

However, finding an energy harvesting technology at a scale of our braking system may seem problematic, since most of them as power cycles have scalability problems.

Thermoelectric generator (TEG), might match our problematic. Indeed its compactness and its need for temperature gradient could be adapted for a breaking system.

Based on this, the problem formulation of my thesis could be:

Is a thermoelectric generator a viable energy harvesting solution for breaks in heavy vehicles?

A group of students composed of *René Haller Schultz, Troels Bartholin Bertelsen and Thomas Helmer Pederson,* has already made a theorical analysis and some numerical models about of the coupling of a break pad and a TEG.

My thesis will therefore focus on an experimental work to confirm or refute the findings of their numerical model

The purpose of this experiment will be to obtain the heat generation measurement, the temperature profile in the pad with or without TEG and the real amount of energy we can get from the TEG under different conditions.

We will then conclude on the viability of using TEG as an energy harvesting system during the deceleration of an heavy vehicle.

3 System presentation

In this chapter the entire setup will be presented and explained. The role of all of its components is going to be explained in order to understand how works this experimental setup . After an overview of the system, we will present in details the most crucial elements such as the braking system, the brake pads and the thermoelectric generator. The purpose of this chapter is to highlight the conditions of the study in order to discuss properly the results.

3.1 The experimental setup

Since this project seeks to prove the interest of our concept and not to develop a marketable prototype, the test bench is made from commercial components. For reasons of simplicity and size, we used components from a VOLKSWAGEN Golf III. This choice is important because as explained before we firstly thought than using a TEG to recover energy from breaking was more adapted to heavy vehicles as trucks. So we will have to think about this when analyzing the results.

The setup is composed of an electrical motor providing angular force to an axle. This axle is then connected to the breaking system, a torque sensor and a flywheel.

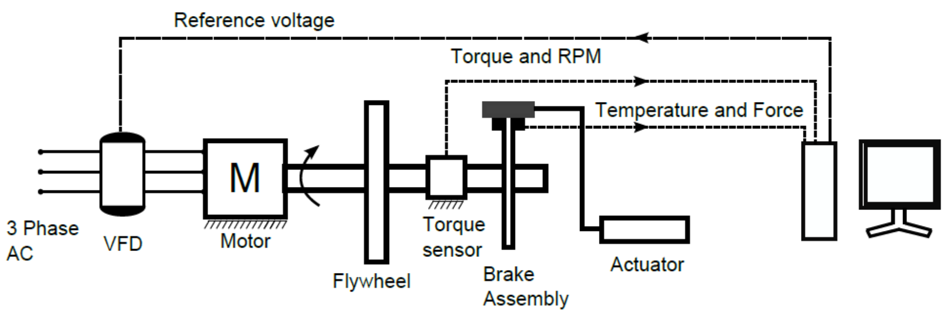

figure 3.1 The experimental setup

The motor is able to provide the speed needed for the reproduction of common situations for road vehicles. So we will have the opportunity to test our system under conditions close to real as an urban driving cycle or emergency braking at different speeds. Since the electrical motor needs high current, we will use a Variable Frequency Drive (VFD) to control the power supplied to it.

The flywheel is used to give inertia to the system. Indeed, to have realistic conditions, the experimental setup must have the same dynamic behavior as the one of a vehicle. To do so, the experimental setup must be able to accumulate as much kinetic energy as a typical car. As the modeling made in the first part of the study, the experiments are carried out considering a single brake assembly. We assume that a car brakes evenly on all four wheels. Therefore, the kinetic energy of the experimental setup is that a quarter of the vehicle. This simplification may seem crude, the front wheels in general producing more stopping power due to weight transfer. However We can afford such a simplification, because the project goal is simply to prove that our concept works. As explain before the braking system is from a VOLKSWAGEN Golf III, the flywheel provides therefore the inertia of a quarter of a Golf III.

A Lorenz Messtechnik DR-3000 and the software Lorenz Messtechnik DR-USB are used to measure the rotational speed of the axle.

To end this global presentation the most crucial component of the setup is the braking system, this element is going to be presented in details in the next part.

figure 3.2 picture of the experimental setup used to carry out the experiments

3.2 The braking system

As specified above, The braking system for the study case is a disc brake system coming from a Volkswagen GOLF III. It is composed of a disc fixed to an axis, two plates, a caliper, a clevis attached to the base frame and a piston subjected to pressure from an hydraulic cylinder.

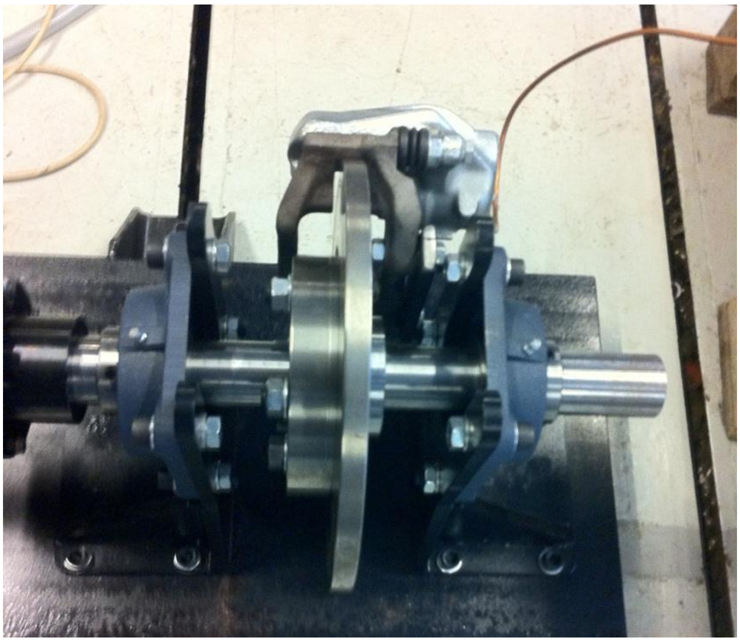

figure 3.3 picture of the braking system

This system is more precisely a floating caliper disc brake. On this mechanism, only the inner pad is pushed against the disc by the piston. The pressure of the outer pad against the disc is carried through the caliper mounted on a slide system in the yoke.

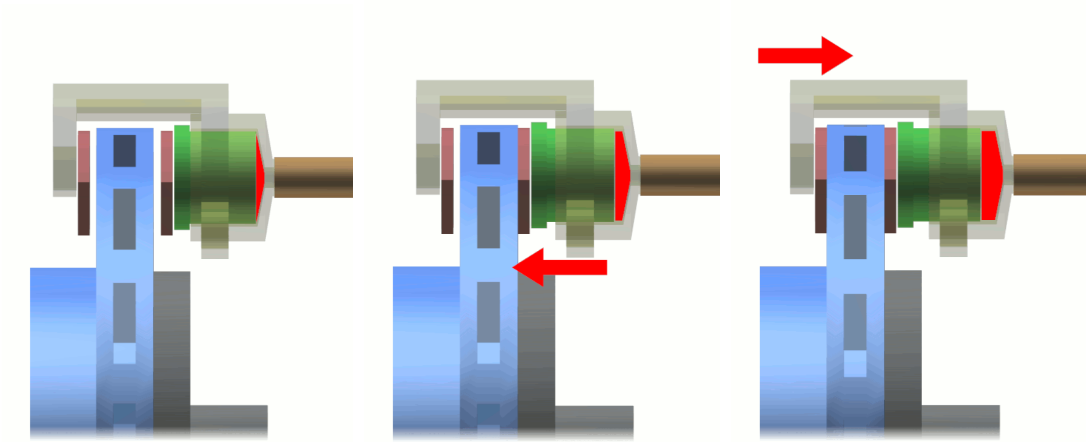

figure 3.4 behavior of the system while braking

With this schematic figures we can observe how is functioning the mechanism. When a sufficient pressure is exerted by the hydraulic jack on the piston, it sticks the inner brake pad to the disc. If the pressure increases, the movement of the piston leads to a movement of the caliper in the opposite direction to stick the second brake pad to the disc.

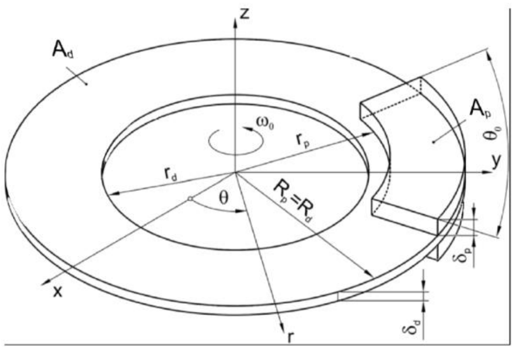

figure 3.5 Sketch of the braking system and the coordinate system orientation

This figure shows us all the important parameters of the braking system and the two coordinate system useful for the study.

The different dimensions and properties for the braking system are presented in **table 3.1.**

	Disc	Pad
Outer Radius [m]	Rd = 0.082	Rp = 0.082
Inner Radius [m]	/	rp = 0.128
Thickness [m]	δd = 0.012	δp = 0.0165
Density [kg.m-1]	7870	2100
Conductivity [$W.m^{-1}.K^{-1}$]	43.5	2.3
Specific heat [$J.kg^{-1}.K^{-1}$]	445	800

table 3.1 Dimensions and parameters of the braking system

It seems important to mention that due to a manufacturing problem of the support, our brake pads are not perfectly coaxial with the disk. However, this slight default should not disturb the measurements because the braking surface remains substantially the same. We will have the opportunity to check the influence of this default in the first sets of experiments. Like this we will be able to ensure that no major disruption is to expect.

3.3 The brake pad

The brake pads are some of the most essential elements of the system. Indeed it is in the pads that we will place the TEG and temperature sensors. So we will be able to study the distribution of temperature in these pads under different conditions and in different situations. To properly analyze the results it is then essential to know the geometry of these elements.

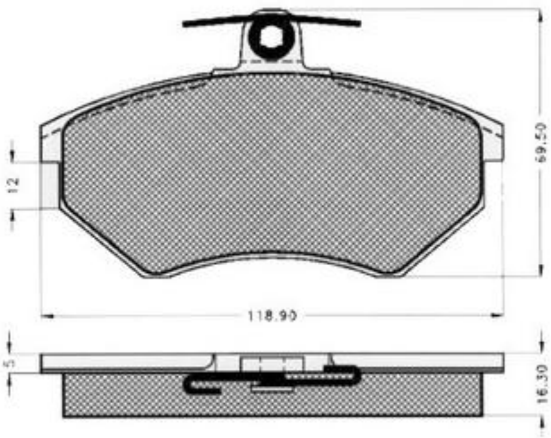

figure 3.6 picture of the brake pad

figure 3.7 dimensions of the brake pad

As shown on figures 3.6 and 3.7, the pad is composed of a 5 mm thick metal base and a 11.5 mm layer of ceramic which provides all the braking characteristics.

During our experiments we will have the opportunity to make some changes on these pads to try to determine the most favorable configuration to recover energy. As shown in **Figure 3.8** we will manufactured the brake pad ceramic to insert the thermo-electric generator and some metal blocks to increase the thermal conductivity.

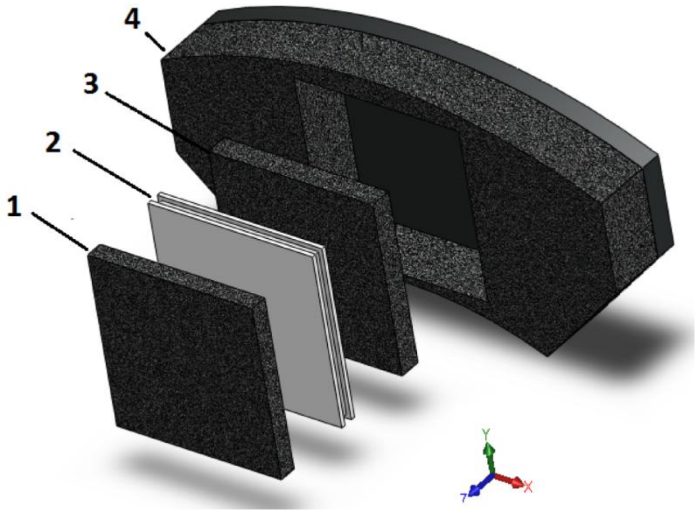

figure 3.8 a CAD of the different modifications of the brake pad

(achieved by Rene Haller Schultz, Troels Bartholin Bertelsen and Thomas Helmer Pederson for the theoretical part of the project)

In the figure the numbers corresponds to:

1: The heat source leading the heat from the braking interface to the TEG.

2: The TEG.

3: The heat sink leading the heat from the cold side of the TEG to the metal base of the pad.

4: The brake pad

All the characteristics of the heat source and sink will be developed in the section dedicated the relevant experiments.

3.4 The Thermoelectric Generator

The TEG used in this project is sponsored by Alpcon, and consists of bismuth telluride doped legs sandwiched between two isolating ceramic plates as shown in figure 3.9.

figure 3.6 The TEG module sponsored by Alpcon.

As presented before, the TEG use the Seebeck effect to produce electricity from a gradient of temperature. It consists of pairs of semiconductor materials (a p-type and a n-type) connected electrically and forming thermocouples. They are then sandwiched between two ceramic wafers. When a temperature gradient is applied between this two wafers, this device generates electricity.

The size parameters of the thermo-electric generator are given in table 3.2.

Surface area	40 mm x 40 mm
Ceramics' thickness	1 mm
Legs' Length	2 mm
Total thickness	4mm
Legs' cross sectional area	2.5 mm x 2.5 mm
Number of pairs	82

table 3.2 Dimensions and parameters of the TEG

3.5 The Data acquisition

For the experiments, a variety of equipment is used to measure the interactions when applying the braking force.

The measurement of the temperatures in the brake pads is achieved by using an array of thermocouples Type K. To perform the cold junction correction (CJC), the thermocouples are connected to an array of AD595AQ. This integrated circuit effectively takes care of the CJC and provides a linear output of 10mV/K.

An acquisition software, National Instruments (NI) LabVIEW 2011, is used to read the voltage signals from both the thermocouples and the TEG. the interface between LabVIEW and the AD995AQ is made by a bus-powered NI USB-6215.

As explained before the rotational speed of the axle is measured by a Lorenz Messtechnik DR-3000. The RPM of the axle is measured using Lorenz Messtechnik's proprietary software, DR-USB-VS.

The braking force is calculated from the pressure applied by the jack to the braking system which is measured by a pressure sensor.

4 Radial and azimuthal heat profile study

4.1 Experiment presentation

This chapter is going to be focused on the heat distribution in the length and the width of the brake pad. These studies have two main purposes. The first one is to confirm the heat profiles found by the modeling analysis in the first part of the project. These profiles don't have a direct influence on the energy recovery but are essential to obtain the heat behavior in the pad during a braking. Knowing them will allowed us to proposed different configurations for TEG's insertion. These profiles will help to discuss the size, the number and the position of TEGs in the brake pad to have the best ration between heat generation and braking efficiency.

The second main goal is to check if the manufacturing default of the support can have any influence on the heat generation geometry and then ensure that our experimental setup remain reliable.

For these experiment we have focused on the Radial and Azimuthal dimension of the brake pad corresponding to the X and Y axis on the **figure 4.1**.

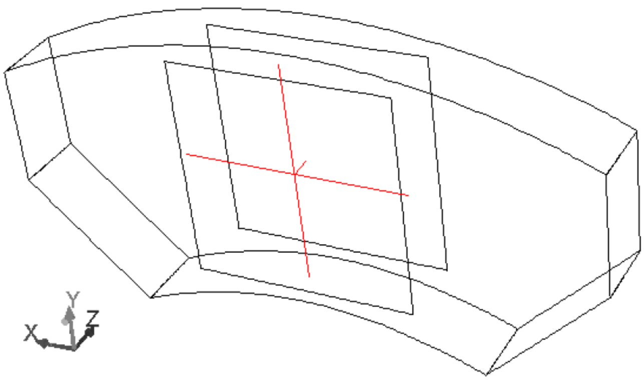

figure 4.1 Axis for the temperature distribution profile

For these two experiments we have used an unmodified brake pad, in which we have drilled some 1,5 mm diameter holes in order to put the thermocouples at 3mm from the pad's hot surface.

The motor was running at 698 $tr.min^{-1}$ corresponding to 5O $km.h^{-1}$ for a wheel diameter of 34 cm. Once the speed reached a braking pressure of 10 bars we have putted on the brake disc for 30 seconds.

During the braking phase, the temperature was picked up every two seconds by the thermocouples. We will carry out this experiment four times in order to minimize any measurement error. We have then plotted the average temperature of all the measurement points after 4, 10, 20 and 30 seconds.

All these experiments were carried out following the method suggested by **[Douglas C . Montgomery, 2005]**.

Using thermocouples allowed us to measure the temperature inside the pad without making any big interventions able to modified its characteristics. But this method does not allowed us to get the temperature of the side of the pad. We will then only discuss the temperature profile inside the pad without boundary conditions.

4.2 Radial heat profile experiment

As explained above, this experiment's purpose is to find a temperature distribution on the radial dimension of the brake pad. To do so four thermocouples were placed inside the pad as shown in **figure 4.2**

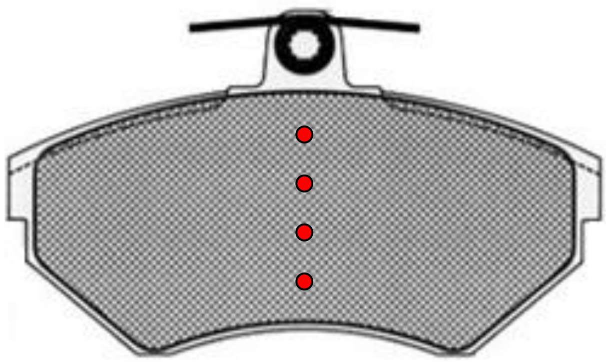

figure 4.2 Radial measurement point distribution

This experiment was performed four times to get reliable results, the curves were then plotted from average values of measured temperatures. Due to a default on the cold junction compensation printed circuit, a few number of the values were inconsistent and so had to be removed has advised in **[Douglas C . Montgomery, 2005]**. All the temperatures measured during this experiment and their average values are available in **Appendix 7.1**.

The plots of the average temperatures after 4, 10, 20 and 30 seconds are shown in **figure 4.3**.

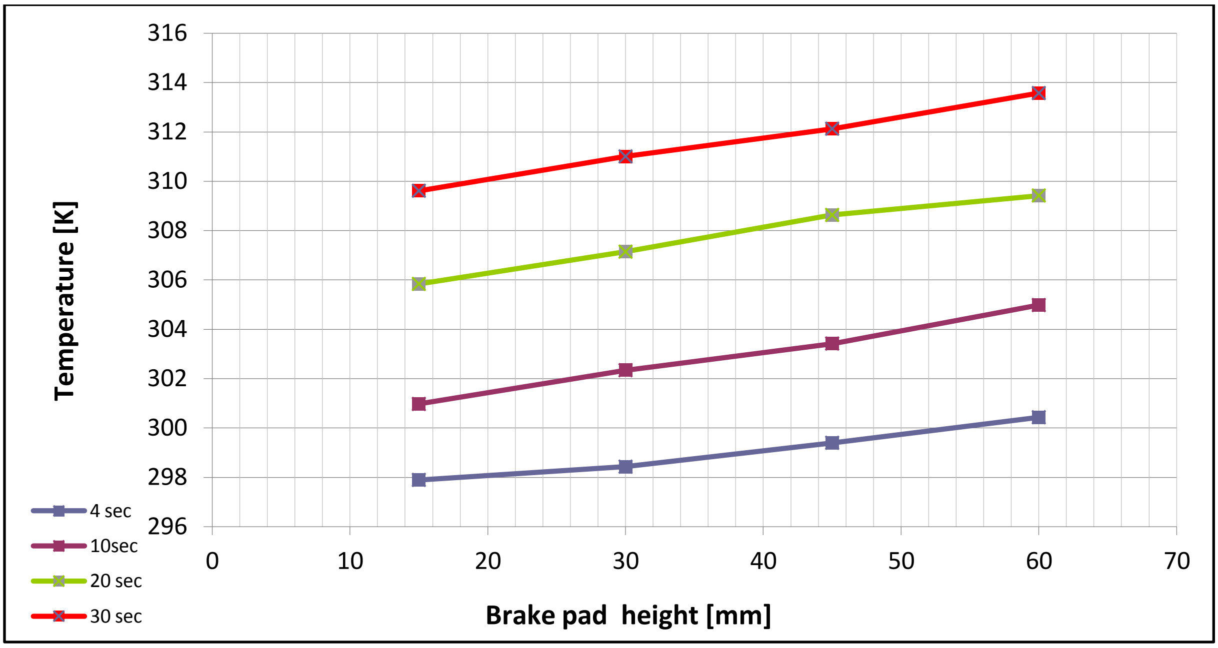

figure 4.3 Radial temperature distribution profile

In this figure we can see that the temperature increases steadily in the pad over time. But this increase is moderate (around 15 K) compared to the amount of energy released during braking. This might be due to the low thermal conductivity of the brake pad material compared to the disc one. We can then assume that most of the heat is dissipated in the disc rather than in the pads.

The second important information is the slight increase of the temperature from the bottom to the top of the pad. This profile seems to confirm the modeling results obtained by my fellow students, however the temperatures obtained are widely below their estimations. Furthermore, the increase of temperature is too low (around 4 K) to have a significant impact on the recovery of energy using a thermoelectric generator.

Moreover contrary to what we could expect, the temperature difference between the four measurement points seems to remain nearly constant through the time. This might be explained by the heat diffusion inside the brake pad.

4.3 Azimuthal heat profile experiment

As explained previously, the purpose this second experiment is to find the azimuthal temperature distribution profile in the brake pad. To do so five thermocouples were placed inside the pad as shown in **figure 4.2**

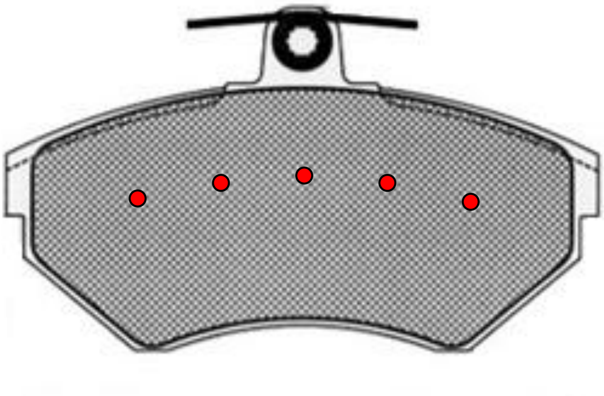

figure 4.4 Radial measurement point distribution

Once again the experiment was performed four times and the curves were then plotted from the average values. All the results of this experiment are available in **Appendix 8.1**.

The plots of the average temperatures after 4, 10, 20 and 30 seconds are shown in **figure 4.5**.

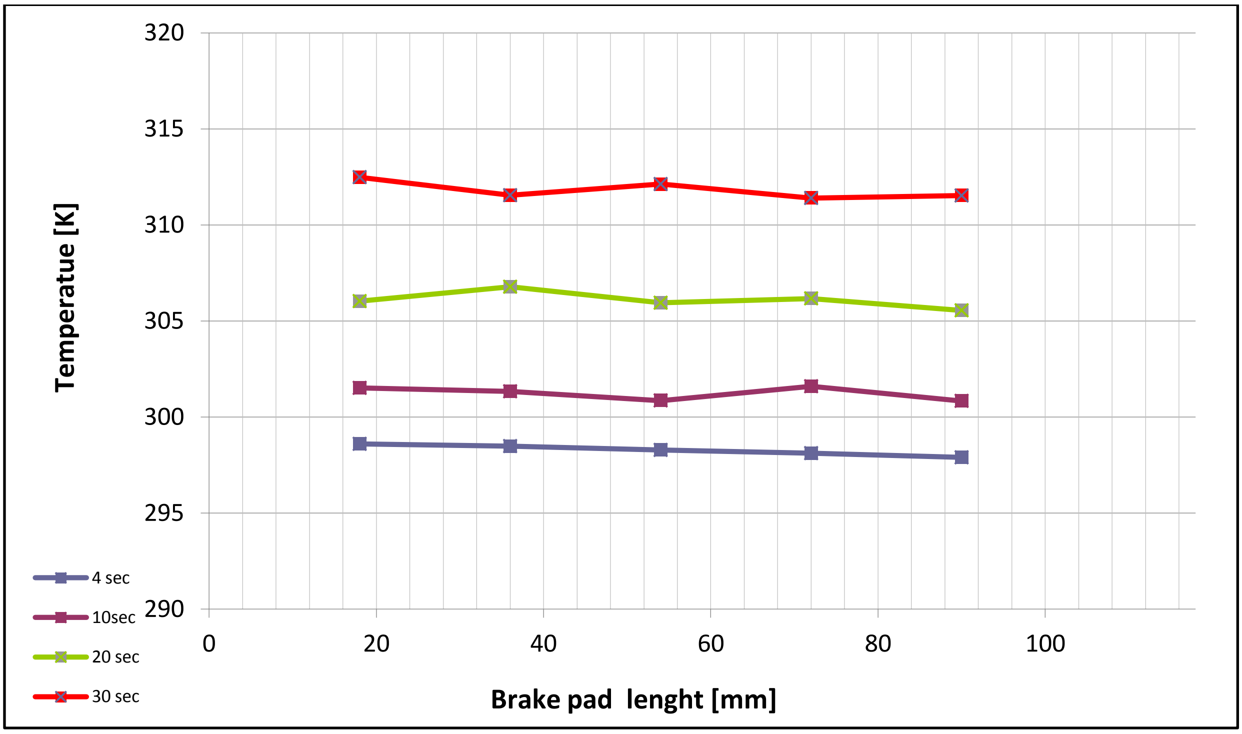

figure 4.5 Radial temperature distribution profile

Like in the radial study, we can observe in this figure a steadily increase of temperature over time. These two experiments have been conducted under the same conditions, so it makes sense that this increase has the same order of magnitude as the previous one.

From the curves, the temperature is quiet constant for all measurement points. The small differences might be explained by the slight inaccuracy of the thermocouples. this result confirms the azimuthal heat distribution found in the modeling study with temperatures much lower than the one of the numerical model.

These two first experiments have shown that the temperature is almost constant in the azimuthal direction and slightly increases radially from the bottom to the top, numerical model distribution is therefore validated by our experimental results but with a big reserve about the range of temperature reached.

These two profile allows us to think about different way to place the TEG. Indeed we can assume that having a large one in the middle of the friction surface worse the braking efficiency. The radial distribution shows us that the temperature is slightly higher in the upper part of the pad, putting one strip of thermoelectric generators close to the bigger radius of the pad would be more efficient and better balance the lost of friction.

We can also now assume than the manufacturing default of the support does not have any incidence on the results. Our setup is therefore reliable to investigate the potential of our concept.

5 Thickness heat distribution profiles

5.1 Experiment presentation

Unlike the previous ones, this set of experiment is not only carried out to validate the numerical results but to have more details on the heat behavior in the thickness of the brake pad. Indeed the main purpose of this is to test a couple of different configurations and modifications to find which ones are the more profitable for the energy recovery. We will therefore make some improvement on the normal pad to increase the heat conductivity and compare the heat distribution profiles to elect the more suitable configuration.

Our experiments are focused on the thickness of the brake pad corresponding to the Z axis on the **figure 5.1**. The numerical study has shown that the thermal conductivity of the brake pad material is too low to recover an interesting amount of energy. Therefore it has been proposed to increase the conductivity inserting metallic blocks around the TEG, as shown in the **figure 5.1**.

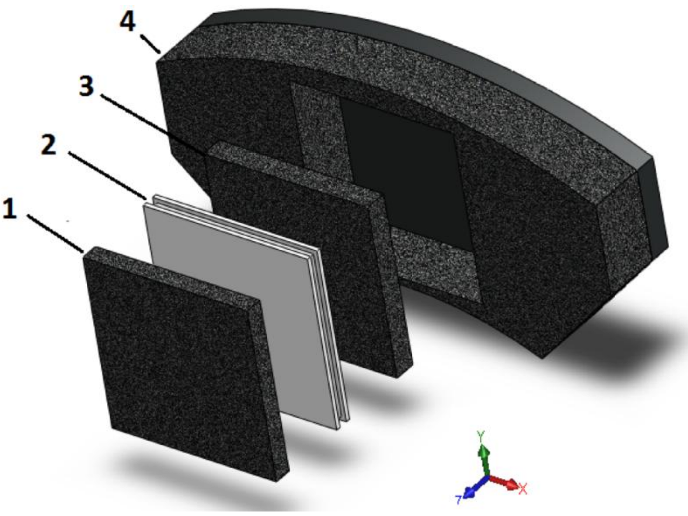

figure 5.1 a CAD of the different modification of the brake pad

In the figure the numbers corresponds to:

1: The heat source leading the heat from the braking interface to the TEG. It is made from a 4 mm thick copper plaque.

2: The thermo-electric generator provided by Alpcon.

3: The Heat sink leading the heat from the cold side of the TEG to the metal base of the pad. It is made from a 5 mm thick iron plaque.

4: The manufactured brake pad. The machining depth obviously varies depending on components used for each experiment.

All the characteristics of the metallic blocks (thickness, material,...) and the position of the TEG have been determinated by the theorical study and the numerical modeling. We will then assume they are the most efficient ones.

For those experiments we are going to drill some 1,5 mm diameter holes in the pad to put some thermocouples every two millimeters. All of them will be at the same depth to avoid the slight temperature difference in the height of the pad, but spread over 4 cm in the length as shown in **figure 5.2**.

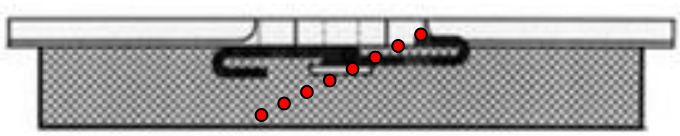

figure 5.2 Measurement points distribution

The motor will be running at 698 $tr.min^{-1}$ corresponding to a 5O $km.h^{-1}$. Once the speed is reached a braking pressure of 10 bars will be applied on the brake disc during 30 seconds.

During the braking phase, the temperature will be picked out by the thermocouples every two seconds. Each experiment will be repeated four times to minimize the measurement error, we will then plot the curves of the average temperatures at different times.

All these experiments and analysis will be carried out following the method suggested by **[Douglas C . Montgomery, 2005]**.

We will first focus on the temperature profile in the unmodified brake pad. The analysis will be very close to the radial and azimuthally ones. Then we will compare in pairs the results for each configuration, to finally conclude on the most adapted one.

5.2 Temperature profile in the unmodified brake pad

As explained above the goals of this experiment are to get a temperature profile in the thickness of the brake pad and to have a base to compare the different configuration results.

As in the two first experiments, the curves have been plotted from the average temperatures after 4, 10, 20 and 30 seconds. All the results and the mean values are available in **Appendix 7.3**.

The curves are shown in **figure 5.3**.

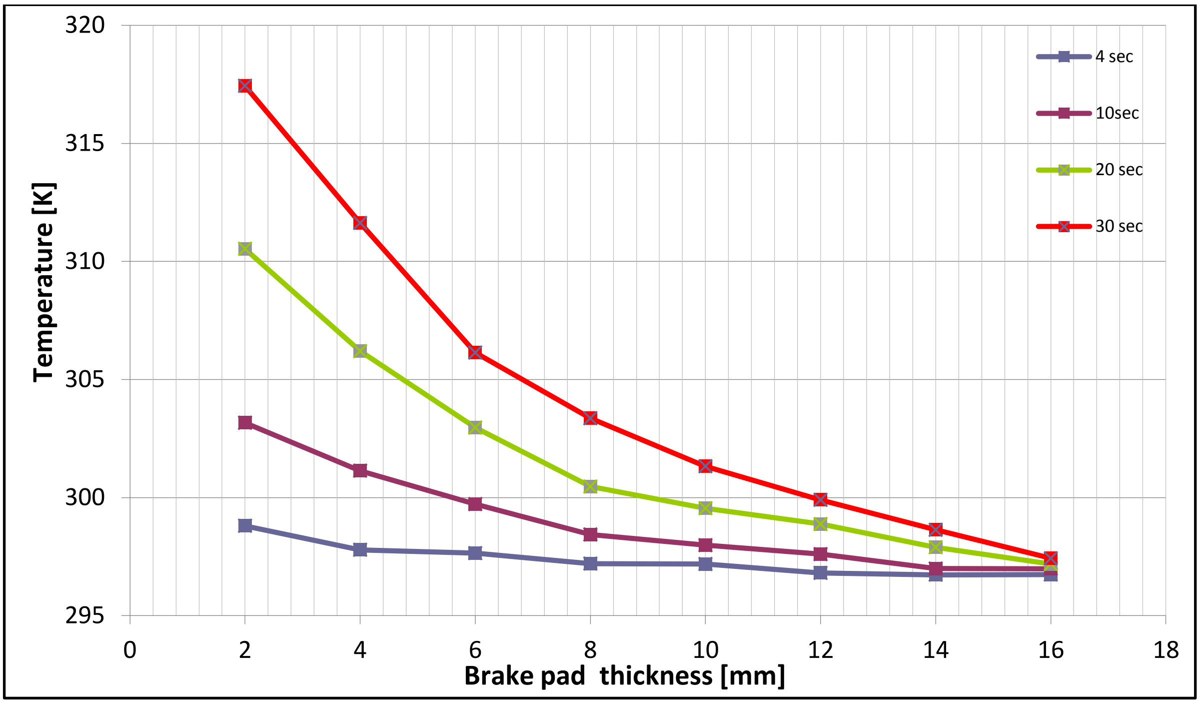

figure 5.3 temperature distribution profile in the thickness of an unmodified brake pad

In this figure we can see that the temperature decreases quickly between the hot and the cold surface of the brake pad. That confirms the low thermal conductivity of the brake pad material.

The maximum temperature of the hot surface have the same order of magnitude than for the two previous studies, which is still too low to recover a sufficient amount of energy.

We can also notice that the temperature of the two last points are very close to the room temperature. The first explanation is of course the low thermal conductivity of the ceramic does not allowed the heat to reach these points. It is as well important to notice that these two thermocouples are located in the metallic wafer with a thermal conductivity much higher than ceramic one. The temperature between these points and the surrounding temperature is therefore logically small.

5.3 Impact of a copper heat source

For this experiment we manufactured the brake pad to be able to put a 4 mm thick copper plaque in it. As shown in **figure 5.4**, it will replace a part of the hot surface of the pad and be therefore in direct contact with the brake disc. Our purpose will be to study the differences in the temperature distribution profile caused by the copper block.

figure 5.4 manufactured brake pad with the copper heat source

All this new set of measurements will of course be carried out in the exact same conditions than the previous one to be able to compare the results properly. All the results and the mean values are available in **Appendix 7.4**. The curves are plotted from the average temperature after 4, 10, 20 and 30 seconds are shown in **figure 5.5**.

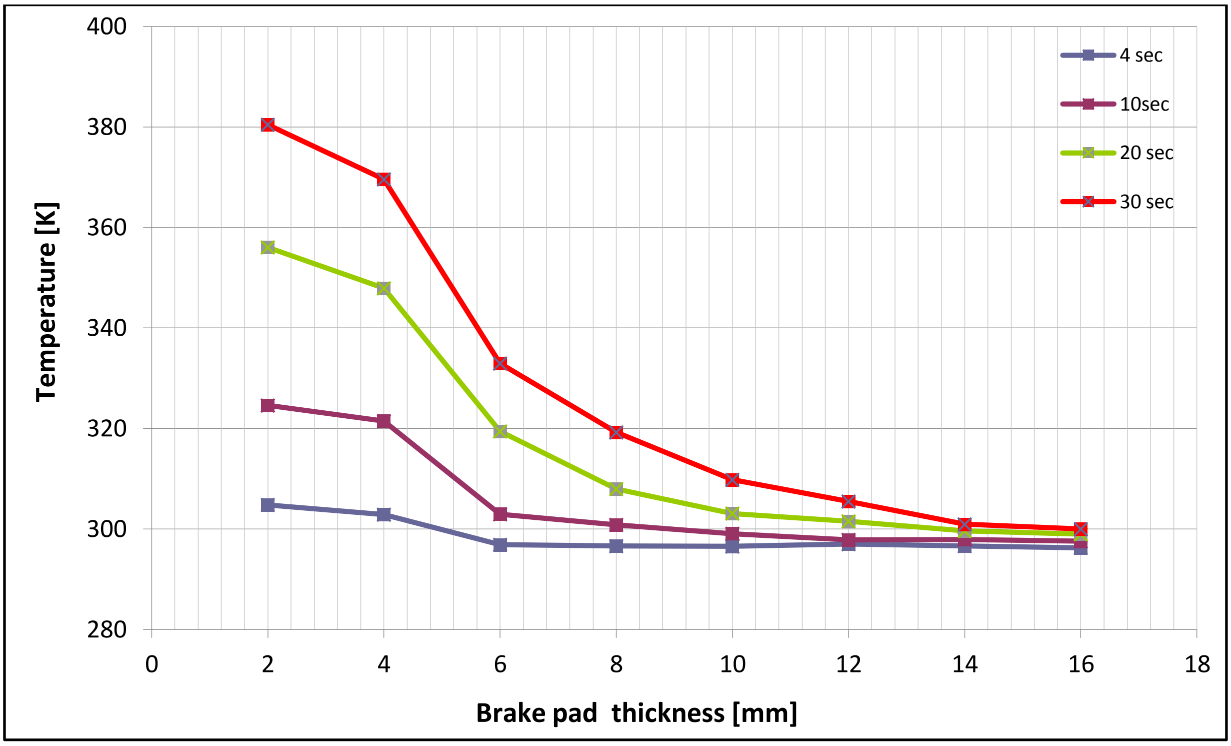

figure 5.5 temperature distribution profile in the thickness of the brake pad with the insertion of a copper block

The first information we get from this figure is the range of temperature reached by the hot surface which is way higher than previously. As you can see the temperature reach 380 K while the one of the unmodified brake pad hot surface was around 218 K. This might be explained by difference of thermal conductivity between the copper and the pad ceramic. In this configuration an important amount of energy goes through the copper while it was previously dissipated in the disc.

The second interesting observation concerns the discontinuity of the temperature profile. Indeed the latter remains very high in the copper and then decreases quickly from the fourth millimeter to the cold surface of the pad. This might as well be due to the difference of thermal conductivity of the materials.

To make a choice between the configurations we have to focus on the area were we will insert the TEG. Higher will be the gradient of temperature applied on the surfaces of the TEG, more energy will be produced.

A comparison of the temperature gradient in the TEG area (between the 4th and the 8th mm) under the two configurations is shown in **figure 5.6**.

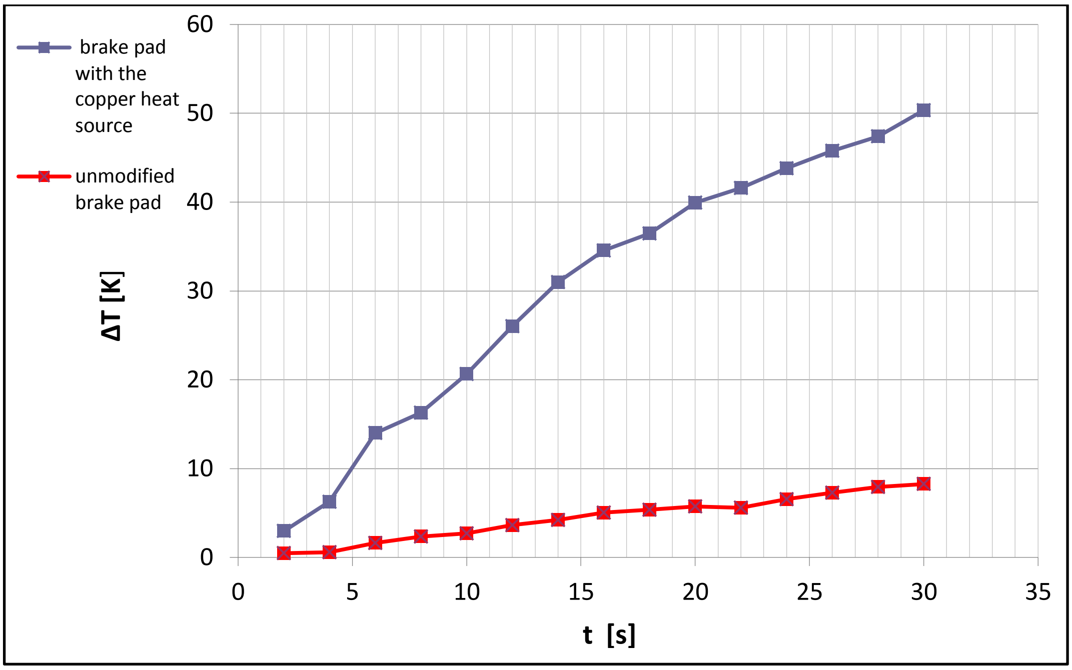

figure 5.6 comparison of the temperature gradient in the TEG area between an unmodified brake pad and one with a copper heat source.

We can see from this figure that the copper block does not only help to reach a more interesting range of temperature, but increases as well the temperature gradient. The difference of temperature between the fourth and the eighth millimeters after 30 seconds is five to six time higher when using a copper plaque as heat source. This is interesting for us because as said previously the energy produced by the TEG depends on the temperature gradient applied between its cold and hot surface. The use of a copper plate seems then justified to recover energy from braking, using a TEG.

We will then choose this second configuration as new base for the next set of experiments investigating the effect of the TEG and the heat sink.

5.4 Impact of the TEG on the temperature heat profile

This new set of experiments will focus on the impact of the thermoelectric generator on the temperature profile. We learned from the previous comparison that the profile is more interesting for the brake pad with a copper block. We will then use thin configuration adding the TEG beside the copper plate as shown in **figure 5.7**.

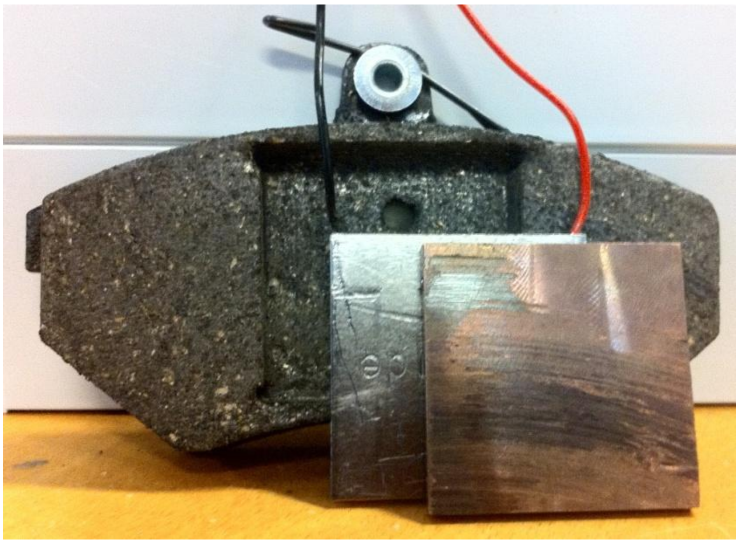

figure 5.7 manufactured brake pad with the TEG and the copper heat source

This experiment will be carried out in the same conditions as the previous ones, the only difference being the number of thermocouples used to pick up the temperature. Indeed it is impossible to drill the TEG, the temperature at six millimeters from the hot surface is therefore impossible to measure. Once again all the results are available in **Appendix 9.5**.

The curves plotted from the average values of the measured temperatures at different depths and time are shown in **figure 5.8**.

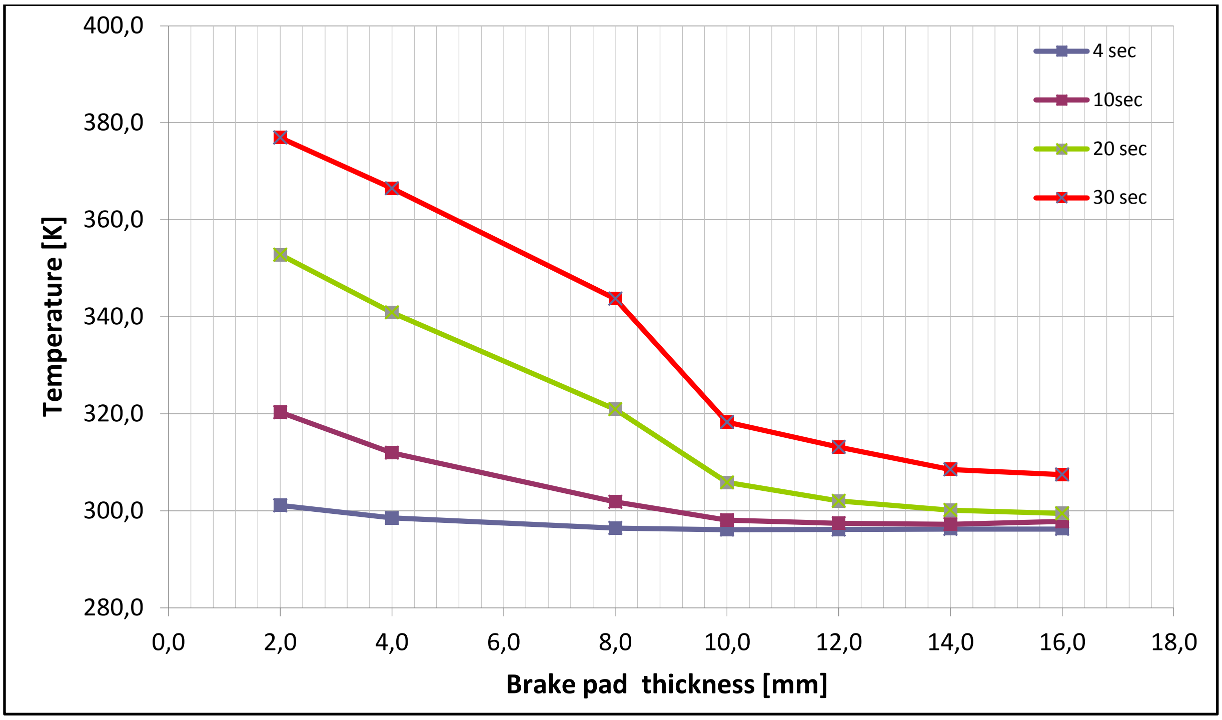

figure 5.8 temperature distribution profile in the thickness of the brake pad with the insertion of the TEG and the copper block

We can see in this figure that adding the TEG in the brake pad does not have any significant impact on the range of temperature reached during the test. However the profile is still slightly different, as the temperature at the eighth millimeter is higher than in the previous experiment. This information is quiet surprising because according to an experiment carried out in the past by the numerical modeling the TEG is supposed to have a low thermal conductivity. Unfortunately this change in the profile decreases the temperature gradient between the two surfaces of the TEG, which is of course worst for the energy generation. Investigating a way to increase the gradient, decreasing the cold surface temperature might then be very interesting.

The rest of the profile shown in this figure (from the 8th mm to the cold surface of the brake pad) seems surprisingly divided in two parts. As the plot shows, the slope of the curve from the eight to the tenth millimeter is way higher than the one of the rest of the curve. This could make us believe that the material change in this area but we know that the iron wafer of the pad only start at the thirteenth millimeter. We will then have a look at the measurement error to see if these surprising results come from a wrong measure or from another problem.

The average, higher and lower temperature measured at 8, 10 and 12 from the hot surface after 20 and 30 seconds are plotted in **figure 5.9**.

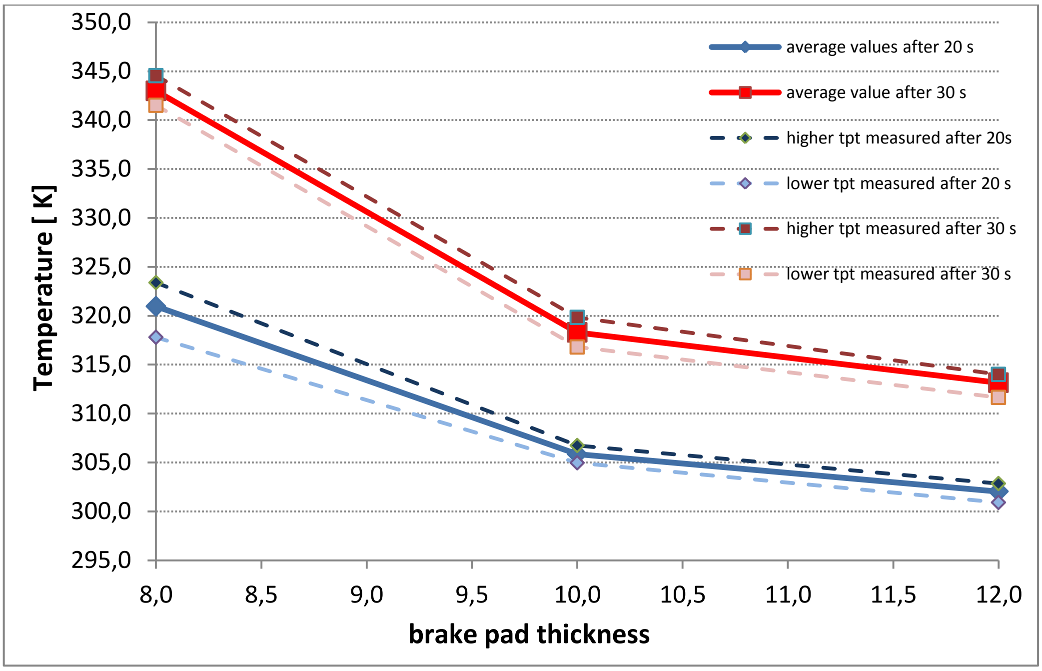

figure 5.9 comparison of the average, the lowest and the highest temperature on the suspect area

This figure shows that the discontinuity of the profile in the area between the eighth and the twelfth millimeter does not come from a wrong measure. The lowest and highest measures are indeed regularly distributed around the mean value.

This surprising curve slope might then come from a problem in the setup. After investigations we assumed that the explanation was a small air gap between the TEG and the brake pad ceramic. The temperatures measured on this set of experiment have then to be taken with caution.

5.5 Impact of an iron heat sink

For this new set of test we will study the consequences of adding an iron heat sink between the cold surface of the TEG and the iron wafer of the brake pad. We will then study the temperature profile in a brake pad including a copper heat source, the TEG and an iron heat sink as shown in **figure 5.10**.

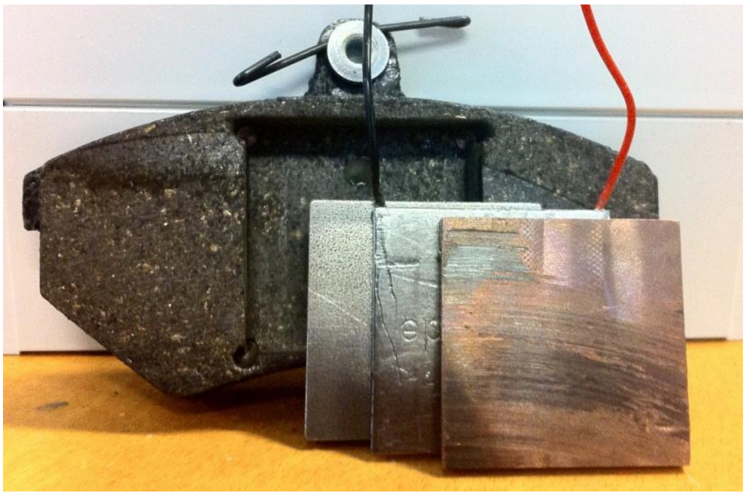

figure 5.10 manufactured brake pad with the TEG and the copper heat source and the iron heat sink

The results of this set of experiments carried out to investigate the impact of the heat sink are available on **Appendix 9.6**.

The **figure 5.11** shows the curved plotted from the mean values of the temperatures measured during this experiment.

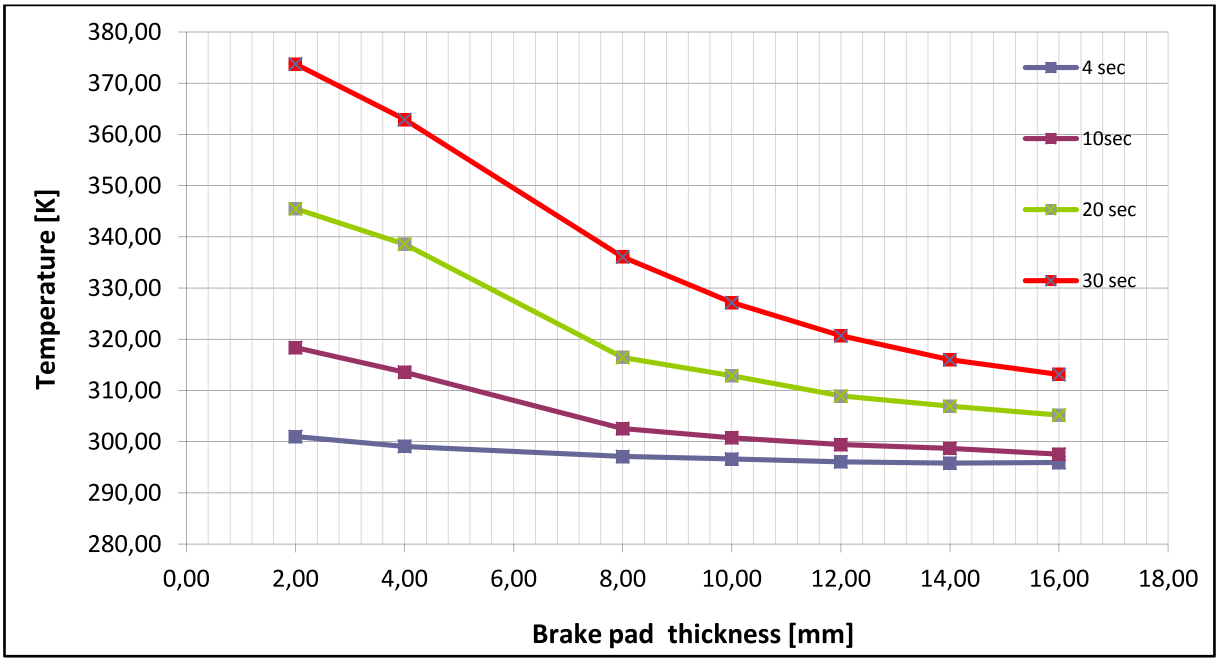

figure 5.11 temperature distribution profile in the thickness of the brake pad with the insertion of the TEG, the copper and the iron block

We can see from these curves that the average highest temperature reached for this experiment is slightly lower than the of the previous sets. This difference is too low to make any conclusions but it might be due to the better heat distribution in the entire brake pad. Indeed we can notice that the temperature of the cold surface of the brake pad is higher than it was for the previous experiment.

We can see as well in this figure the different influence of the thermal conductivity from the three materials. Indeed, we distinguish three different slopes on the temperature curves. The first up to 4mm corresponds to the copper, the second ranging from 4 to 8 mm corresponds to the TEG and the last from 8 to 16mm represents the two layers of iron.

It is now time to compare the gradient of temperature through the time between the two surfaces of the TEG to finally find which configuration is the most efficient for energy recovery.

These temperature gradients between the fourth and the eighth millimeter for the configuration with and without the iron heat sink are plotted in **figure 5.12**.

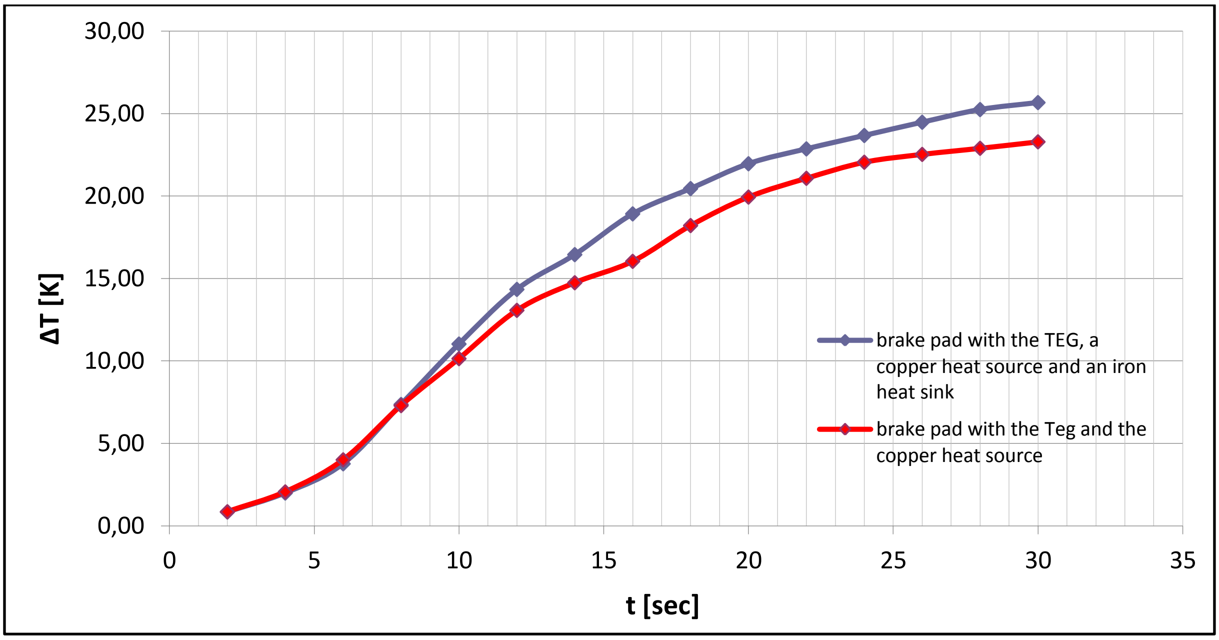

figure 5.12 temperature gradient between the fourth and eighth millimeter through the time, with or without a iron heat sink.

This figure shows us that the temperature gradient between the hot and the cold surface of the TEG is slightly higher when using a iron block as heat sink. Even if the difference is only around three Kelvin, it might have a significant impact on the heat production through the time.

All these experiments and comparisons between the different configuration bring us to the conclusion that the copper heat source and the iron heat sink might improve the energy recovery inside the brake pad. We will then chose the configuration including all these elements to carry out all the next experiments.

5.6 Study of the heating and cooling phases

We already know that the energy recovery depends on the temperature gradient and is therefore not constant in the time. After focusing on the heating phase to determined the most productive configuration of the pad, we are going to focus on the entire thermal cycle which include both heating and cooling phases. This study will allow us to understand the thermal comportment of our modified brake pad through the time to determinate for how long the production of electricity is possible after a braking.

All this set of experiments we will carried out in the same conditions as the previous one. The motor will be turning at 698 tr/min, a braking pressure of ten bars will be applied during 30 seconds. After this period the pressure will be released and the motor switched off. The temperatures will be picked up every five seconds for two and a half minutes.

All the results of the set of experiments and the average temperature values are available in **Appendix 9.7**. The curves of the temperature through the time for the different points of measurement is plotted in **figure 5.13 and figure 5.14**.

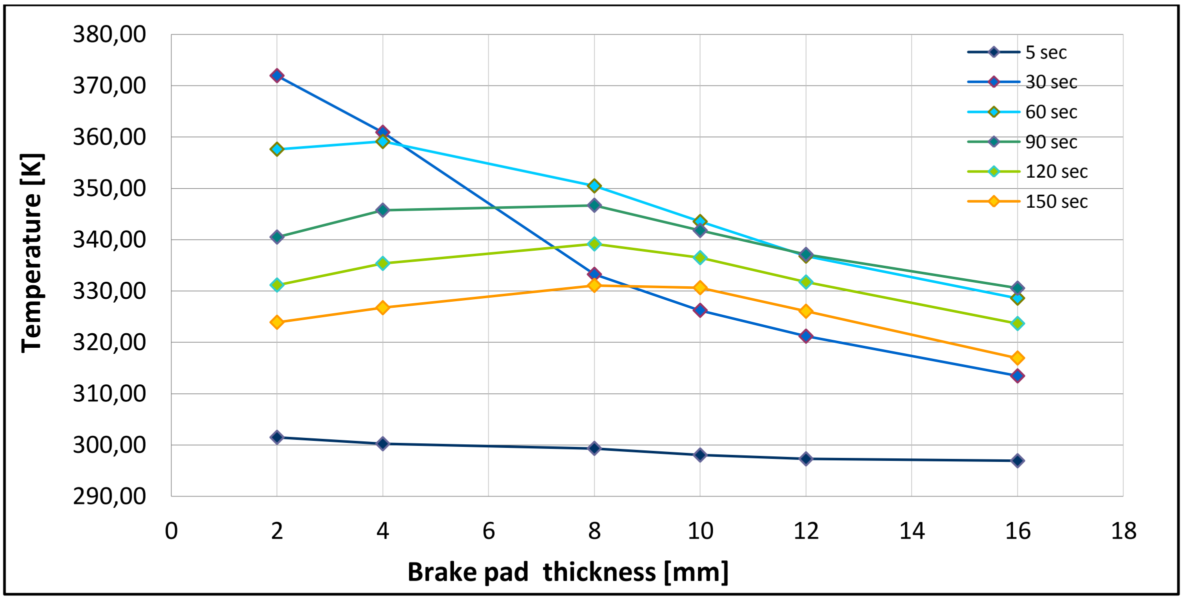

figure 5.13 temperature distribution profiles through the time in the thickness of the modified brake pad

This figure shows us the temperature profiles in the brake pad every thirty seconds The curves plotted after 5 and 30 seconds are similar to previous experiment ones, that shows that the conditions of measurement remain the same. The curves plotted after 60 seconds, thus the end of the braking phase, shows that the heat moves slowly to the cold surface of the brake pad. The higher temperature is now picked up at 4 mm inside the brake pad. The three last curves shows the same trend despite the global decrease of temperature in the pad. After 150 seconds the temperature is found between 8 and 10 mm.

This figure gave us some interesting information but does not help us to know the period of electricity production of the TEG.

The **figure 5.14** shows the temperature evolution for each measurement point through the time.

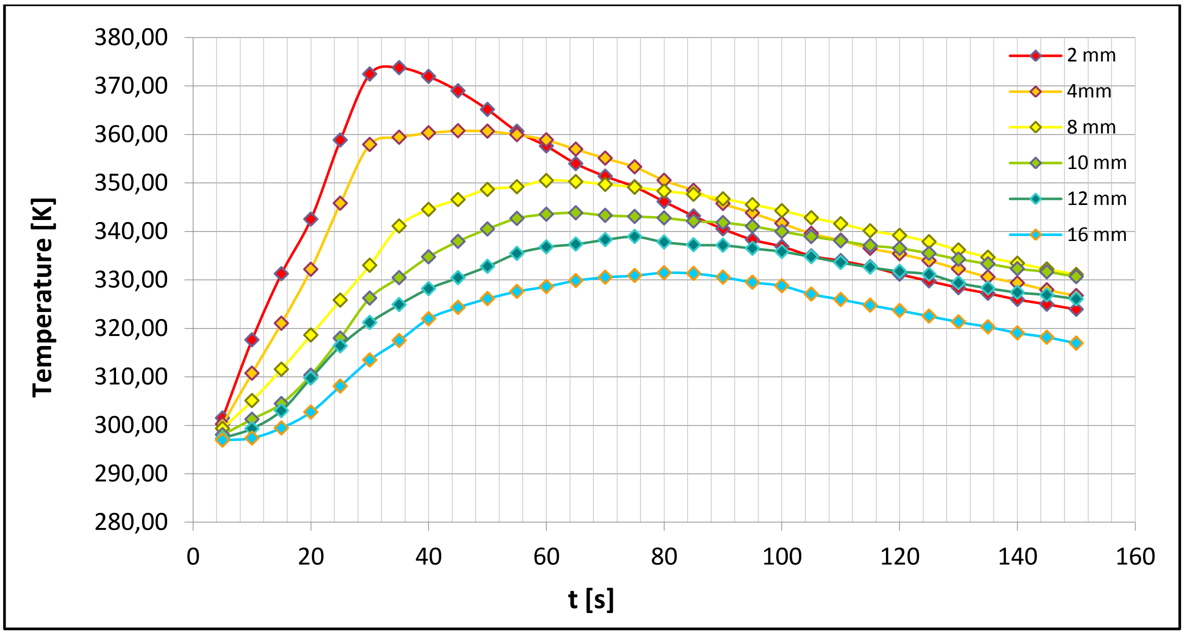

figure 5.14 temperature evolution through the time at different depths of the modified brake pad

Thanks to this figure we can compare the evolution of the temperature at different depth in the brake pad. We can for example see that the increase of temperature is of course more shorter and intense close to the friction area than near the cold surface. The fast decrease of temperature of the hot surface after the braking is due to the convection through the air and the convection through the modified brake pad. Except the last point of measurement all the other ones are only subject to conduction, the evolution of their temperature is then slower.

Of course the most interesting curves are the one for the hot surface of the TEG (in orange) and its cold surface (in yellow). The hot surface remains significantly hotter than the cold one for a period of more or less 60 seconds, this period would then be quite productive for the TEG. After this period the temperature difference decrease and is reversed after 90 seconds.

Let us have a closer look at the temperature gradient between the two surfaces of the TEG plotted in the **figure 5.15**.

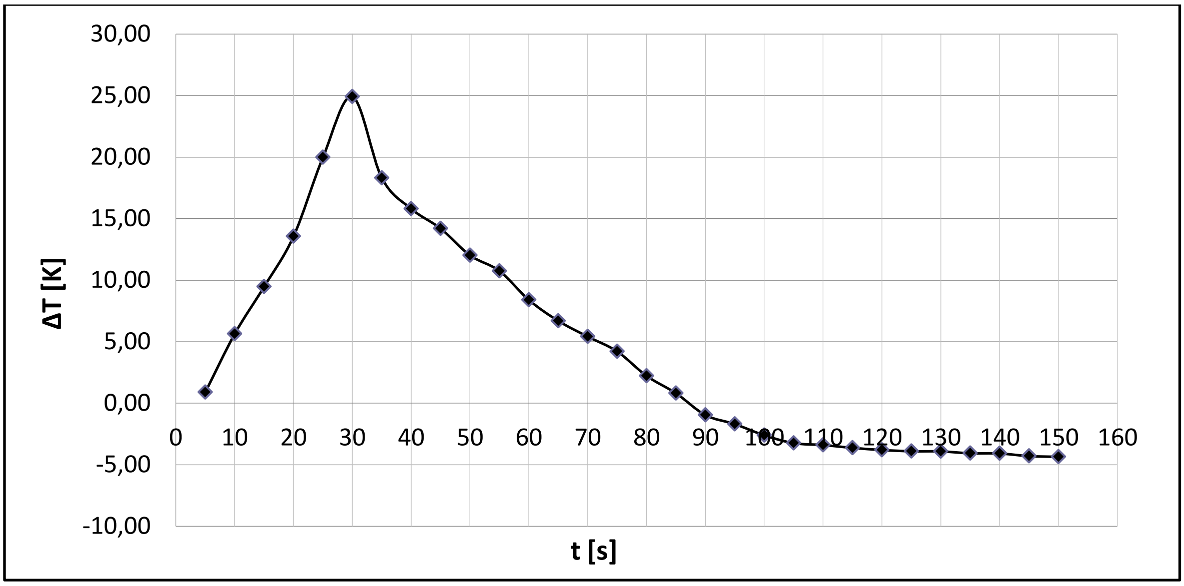

figure 5.15 temperature gradient between the fourth and eighth millimeter through the time

This figure confirms the previous observations made on **figure 5.14**. The gradient increase during all the braking and start to decrease as soon as we stop braking. It reaches 25 Kelvin and then decreases to get reversed after 90 seconds. The gradient is then higher than 5 Kelvin for 60 seconds, we can therefore observe than the productive period is longer than the braking phase.

This entire chapter was dedicated to the study of temperature profiles in the thickness of the brake pad . We first learn that the temperature reached in a normal one was not high enough to recover an interesting amount of energy. We then decided to modify the pads and to compare the profiles with different modifications. Comparing them have allowed us to highlight the usefulness of the insertion of a 4 millimeter copper block and a 5 millimeter iron block, used respectively to lead the heat to the hot surface and to dissipate it from the cold one of the TEG.

We also studied the evolution of the temperature gradient across the TEG over the time. We now have a good idea of the maximum gradient and the period of production available for a constant braking of 30 seconds at 50 km/h.

It is now time to study the energy generation using our modified brake pad under different conditions, to finally conclude on the interest of our concept.

6 Energy recovery study

This chapter is dedicated to the energy production concerns. Its main purpose is to get as much information as possible about to the energy recovered by the TEG. We have first focused on the open circuit voltage produced during different kinds of braking. Then we tried to produce the maximum power production using a resistance as close as possible as the TEG one. With all this results we finally discussed and conclude on the interest of our concept.

All of our experiments have been carried out using the most efficient brake pad configuration including the copper heat source, the iron heat sink ant of course the TEG.

6.1 Open circuit voltage production

This study is composed of five experiments. Each of them reproduces a different driving situation. The first three ones will represent an emergency braking from 30, 50 and 70 km/h. Reaching an higher speed would be interesting but unfortunately unsafe for the experimental setup. The Fourth experiment represents a constant downhill braking. For it we have used the same conditions as in the previous experiments. The last one follows the urban part of the New European Driving Cycle, which is the cycle used to test the car consumption.

For all these experiments the TEG is going to be directly connected to the bus-powered NI USB-6215, to be able to read directly on the computer the open voltage produced by the TEG.

Lets first have a look on our emergency braking experiments. To reproduce the conditions of this braking, we have run the motor at a speed corresponding to most of European speed limits. Once the speed reached, we applied the maximum pressure on the brake. We then picked up the voltage produced by the TEG every seconds.

All our experiments were once again conducted four times to get some reliable results.

Figures 6.1, 6,2 and **6.3** shows the voltage curves for the three emergency braking, all the results are available in **Appendix 9.8, 9.9 and 9.10**.

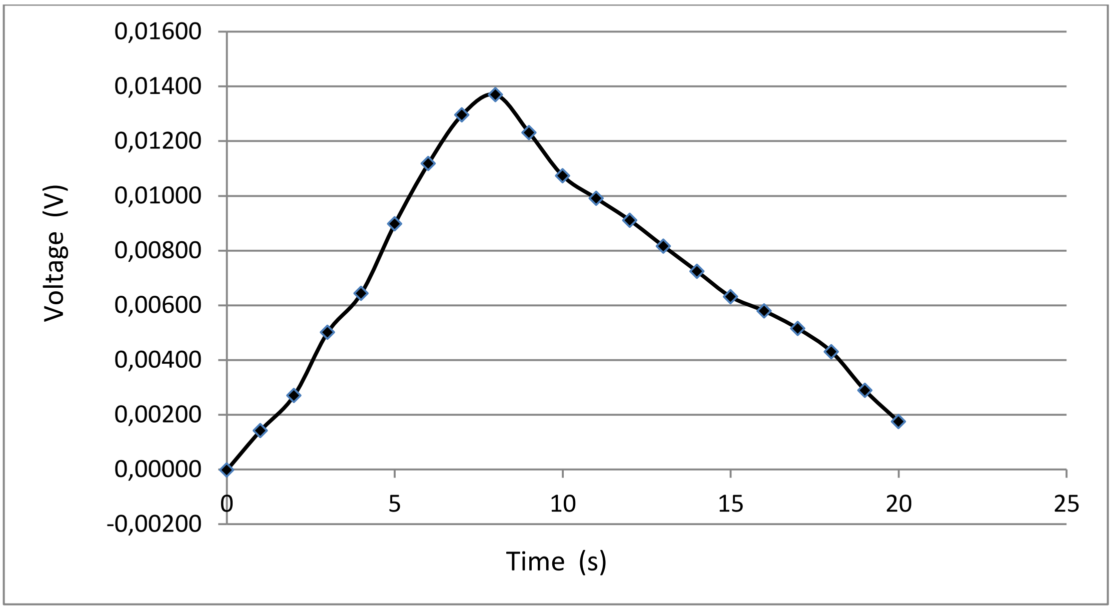

figure 6.1 Voltage produced in open circuit after a 30 km/h emergency braking

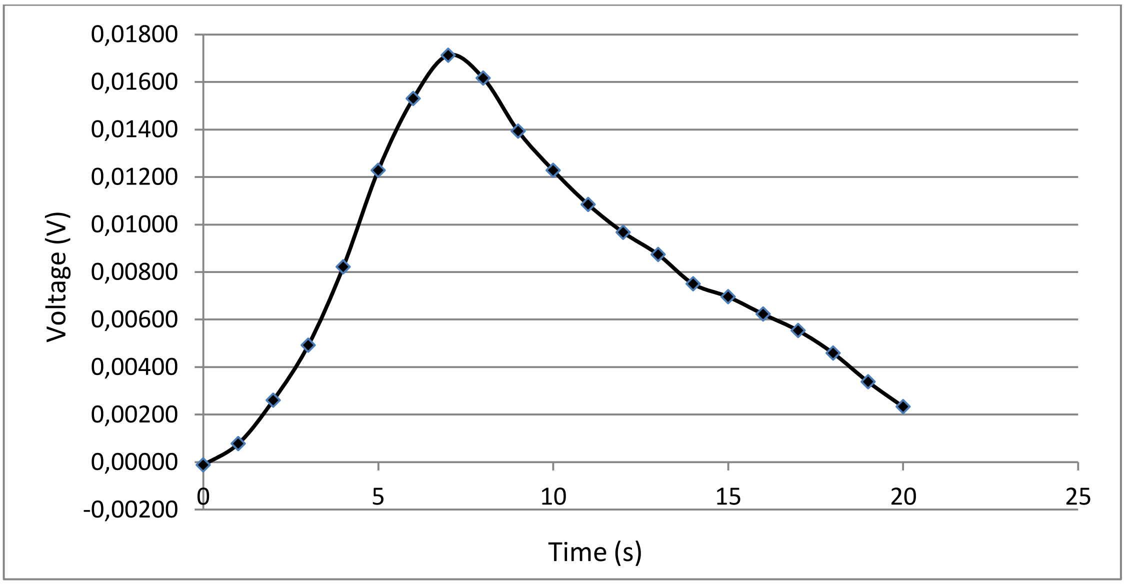

figure 6.2 Voltage produced in open circuit after a 50 km/h emergency braking

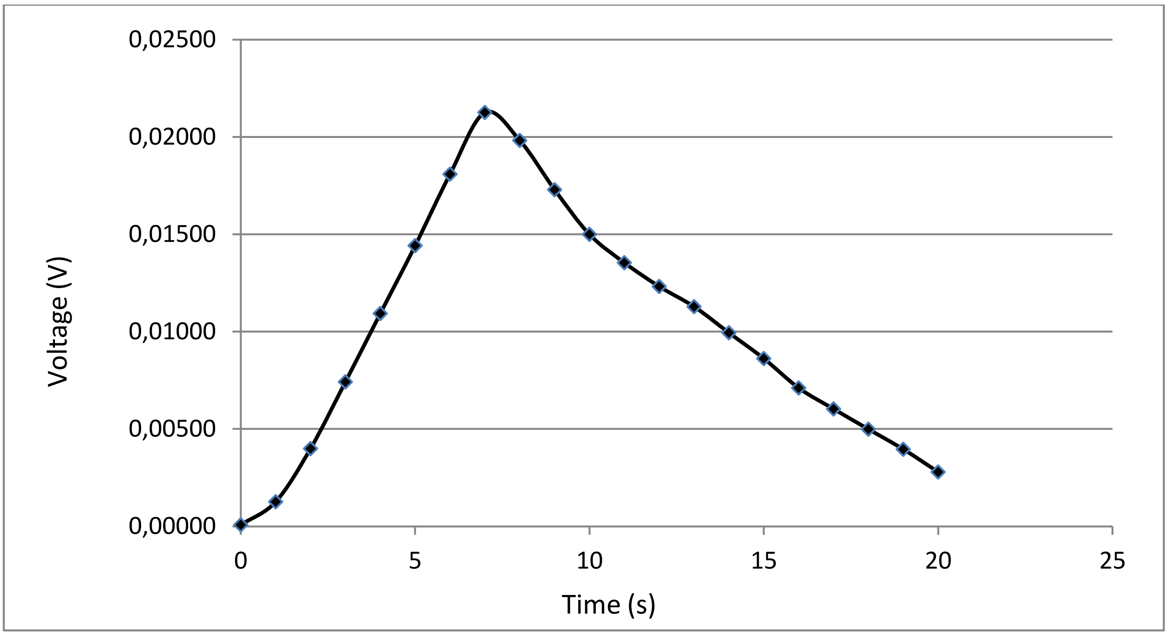

figure 6.3 Voltage produced in open circuit after a 70 km/h emergency braking

These three experiments were really similar, the only changing parameter being the speed reached before the emergency braking. It is then logical to find some close results. In all these figures we can find the same shaped plots, the voltage increases first for 8 to 9 seconds and then decreases with the temperature.

This shape was expected and seems logical, nevertheless, the voltages reached during all these experiments are lower than what we could expect. Indeed, we are studding the open circuit voltage production, the Resistance is supposed to be infinite and the current barely nil. The voltage between the legs of the TEG was then supposed to be quite high. with a voltage this low, can imagine than the amount of energy recovered by the TEG is nearly nil. This phenomena might be due to the insufficient amount of energy brought to the TEG, indeed most of the heat generated by the braking is dissipated in the brake disc.

Even with this low results we can see that the voltage produced after the 70 km/h braking is higher than the other ones. We can then conclude that as expected the kinetic energy lost during the braking have an impact on the amount of electrical energy recovered.

These three experiments shown us than our technology does not seem adapted to middle range vehicles which only brake occasionally. Lets now have a look on the results for a constant downhill braking.

To carry out this experiment we used the same protocol as all the experiment of the previous chapter. We braked continually to maintain a speed corresponding to 50 km/h for 30 seconds.

The voltage produced by the TEG was picked up every five seconds for 120 seconds to be able to study the energy production for the entire thermal cycle.

The **figure 6.4** presents us the voltage production during this constant downhill braking, all the results are available in **Appendix 9.11**.

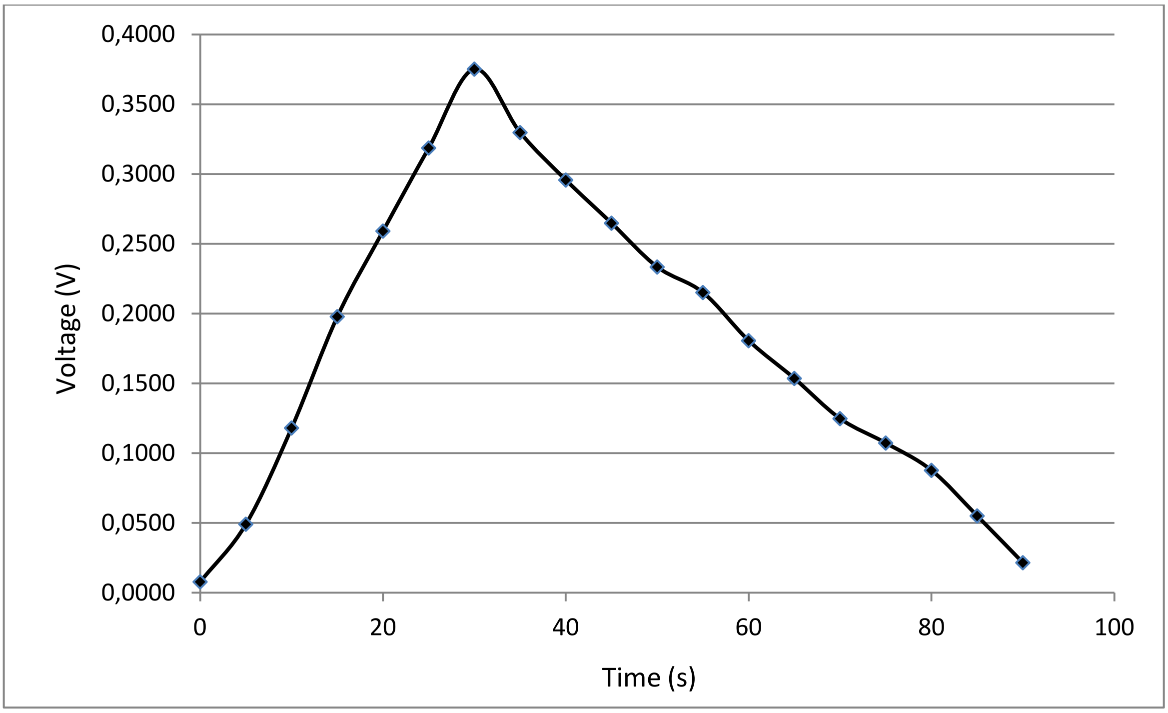

figure 6.4 open circuit voltage produced during a 30 seconds downhill braking

The curve plotted on this figure has the same shape as the three previous ones but this time, the maximum voltage produced by the TEG is around ten times higher. This difference is easily explained by the amount of energy brought to the TEG. We already know that the energy production increases with the gradient of temperature between the legs of the TEG. During this experiment the temperature of the hot surface is way hotter than during the previous ones, the higher voltage production is then logical. Nevertheless the voltage produced by our setup remains lower than what we expected for an open circuit experiment.

Our previous chapter allows us to know the amount of energy brought to the TEG during these 30 seconds and the temperature gradient between its two surfaces. We can then assume that this surprisingly low results must come from the TEG properties.

This last affirmation is confirmed when we have a look at the **Appendix 9.3 "**TEG Output from a Known heat input" of the theorical and modeling part of the project. In this chapter my fellow students founded that when heating the hot surface of the TEG with a 100 W heat film the maximum open circuit voltage produced by the TEG was only around 0,7V. Even if The two experiments' conditions are hard to compare we can see that the order of magnitude of our results seem to match.

To finish this open circuit study, we focused on the production during an urban driving cycle. As presented before we have tried to replicate the urban part of the New European Driving Cycle. The NEDC is the cycle used to calculate the consumption of every car sold in Europe. This experiment will then allows us to know the voltage production of our TEG under realistic driving conditions. During this test we will focus on the Urban part of the cycle because the two others parts don't present any interesting braking phases.

This urban part corresponds to the first 800 seconds of the cycle NEDC shown on **figure 6.5**.

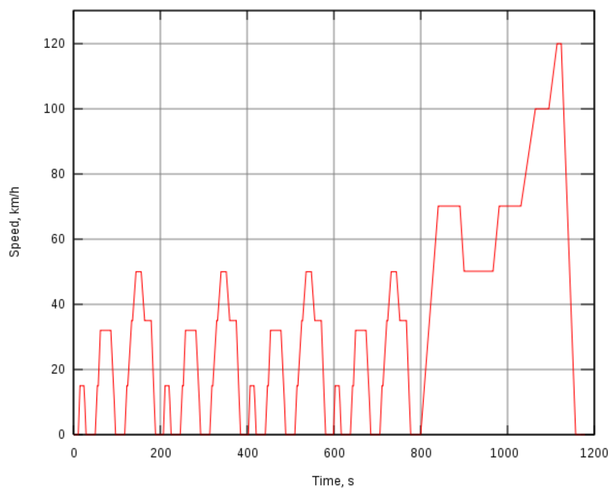

figure 6.5 New European driving cycle plot

As shown in the figure, The urban part of the NEDC is composed of twelve accelerations and braking phases divided in four identical smaller cycles spread out on 800 seconds. To allow us to study all the voltage production during this test we will continue to run the experiment for 100 more seconds of cooling time.

To be as close as possible from the NEDC, the braking pressure was putted slightly on the brake disc to decrease slowly the speed but for some material reasons the acceleration phases were a little bit faster than they were supposed to be. However, this difference should not have any impact on our results, indeed only the braking phases have some influence on the heat generation. Unlike during the constant downhill braking experiment, the motor was switched off at the end of each acceleration phase and only the brakes were used to control the speed during the deceleration phase.

During all the experiment , the output voltage have been picked up every five seconds. For some reasons of time this experiment have only been repeated two times, All the results are available on **Appendix 9.12**, the voltage curve is plotted in **figure 6.6**.

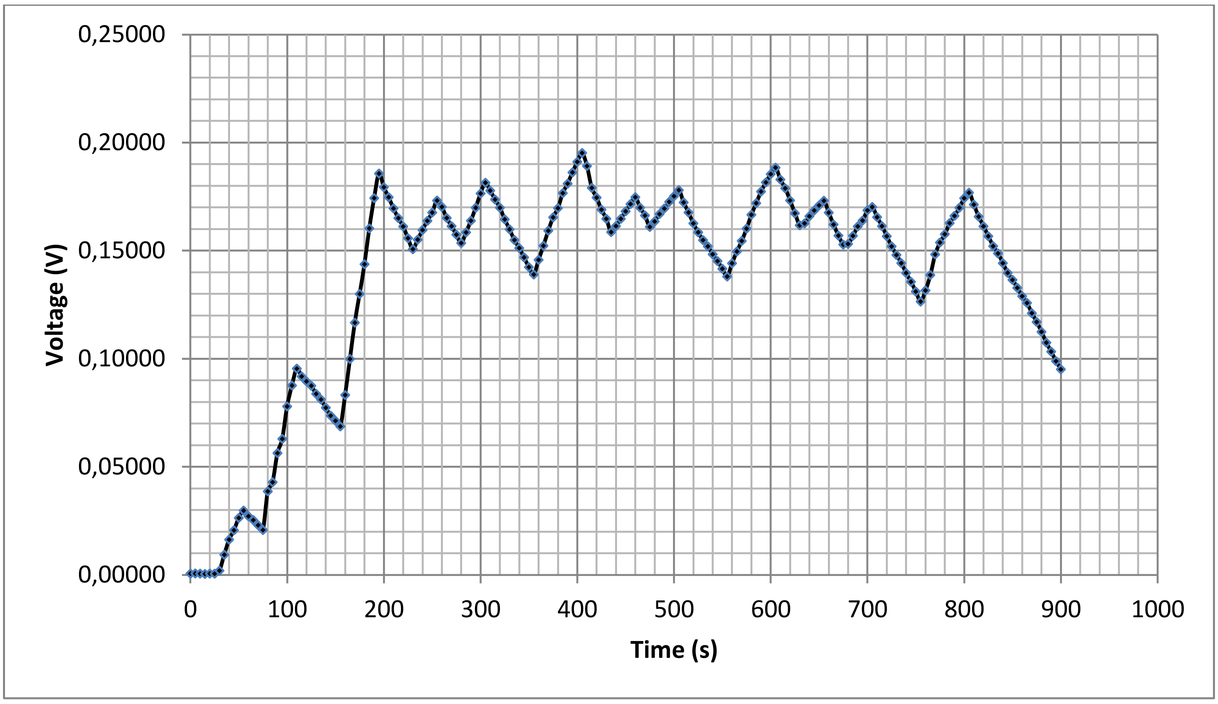

figure 6.6 Voltage produced in open circuit following the NEDC urban cycle

This figure is really interesting because it gives us a lot of different information.

Firstly it is important to describe the shape of the curve to locate the main information. The first 25 seconds correspond to the first acceleration, this phase does not have any influence on the voltage since the pad bake is still at the room temperature. We can find the first cycle corresponding to the main increase in voltage from 30 to 200 seconds. As we could expect each cycle is composed of three peaks, with the higher corresponding to the 50km/h braking.

If we have a look at the maximum output voltage we can see that it is lower than the constant downhill braking one. This makes sense because the energy brought to the TEG was only equal to the kinetic energy lost during the braking while it was previously provided by the motor.

If we focus on the cycle repetition, we can see that after the second one, the higher voltage reached for each peak is slightly lower than in the previous cycle. This result could seem surprising because we can assume that the temperature of the brake pad increases through the time. But it is important to keep in mind that the output voltage is only dependent of the gradient of temperature.

We can then imagine that after a certain time, the average cold surface temperature increases more than the hot surface's one. Improving the cooling of the cold surface would then be essential to recover more energy for a long driving time.

6.2 Power and energy concerns

In this last chapter we have been focus on the power and energy production by the TEG. We chose to carry out this last experiment with a constant downhill braking because this situation seems to be the most productive one.

To study the power production of the TEG we had to apply a resistance between its legs. In order to maximize this production, the resistance have to be equal to the TEG's one, which increases with the temperature. We then made the choice to use a variable resistance, but to make our final choice we had to study the TEG's resistance during the braking.

For this purpose, we used a thermocouple placed at 2mm from the brake pad hot surface and a ohmmeter to find the relation between TEG resistance and temperature.

The curve of the TEG's resistance in function of the temperature is plotted in **figure 6.7**, once again all the results of this chapter are available in **Appendix 9.13**.

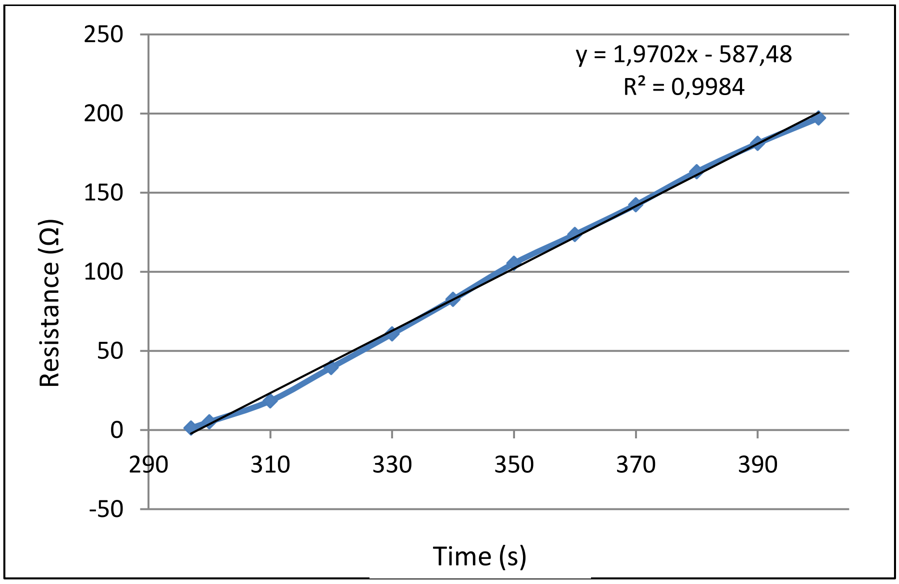

figure 6.7 Resistance of the TEG in function of the temperature

Thanks to this figure we can see that the resistance of the TEG increases linearly from 1 to 200 Ω between 300 and 400 K. We then chose a variable resistance of the same order to carry out our experiment.

We can see as well that the resistance is really close to the tendency curve of equation:

$$y= 1{,}9702x - 587{,}48$$

Thanks to this equation we made a table of correspondence between temperature and TEG resistance helping us to modify the circuit resistance during the experiment. The resistance changes was made following this table, manually using the variable resistance and a ohmmeter. A manual control of the resistance is less accurate than an automatic one, but the goal of the experiment is just to have a good idea of the maximum TEG power production. Using a complex automatic control system would require way more time and would then not be justified for our study.

During the 90 seconds of experiment we picked up the temperature and The voltage every 5 seconds using the software Lab View and its interface NI-USB 6215.

The power output was the founded using the next formula:

$$\mathbf{P= U^2/ R}$$

with P: power (W), U: voltage (V) and R: equivalent resistance (Ω)

The curve of the Power output through the time is shown in **figure 6.8.**

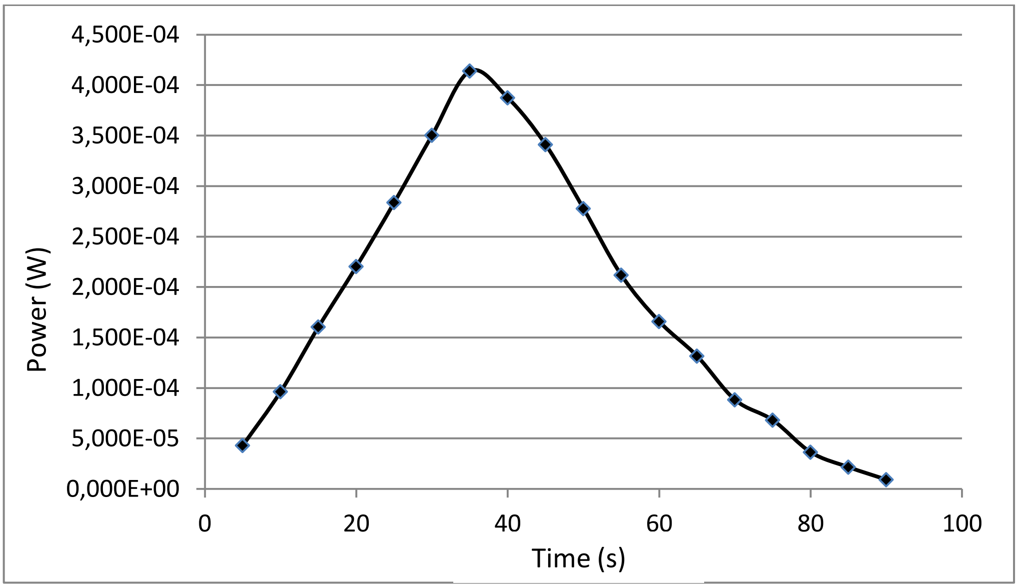

figure 6.8 power produced during a 30 seconds constant downhill braking

We can see in **Appendix 9.13**, that as we could expect the voltage generation is lower than the open circuit one but have a similar shape. It reaches a maximum around the end of the braking phase and decreases during the cooling one. This figure shows that the power generation profile follow as well more or less the same shape.

But the most important information provided by this experiment is the low amount of energy recovered by the TEG. Indeed the average power production during this 90 seconds is 0,19 mW which represents a total energy recovery of 0,017 Joules. This result is very low and is mainly explained by the low TEG's voltage output which was never higher than 0,2 V.

These energy recovery results are way lower than all the results founded in the modeling section. Mainly because they expected an higher gradient of temperature between the two surfaces of the TEG. In their **chapter 7** "modeling results" their power results were obtained for a TEG's surface gradient of 300 K, which is of course impossible to compare with the gradients founded in our experimental study.

7 Final discussion and conclusion

The main goal of this project was to investigate and experiment the recovery of energy from a brake pad using a thermoelectric generator.

After this experimental study, I must say then I share most of opinions given after the modeling analysis. Indeed it seems obvious that our TEG is not adapted to our conditions in order to recover an interesting amount of energy. But unlike my fellow students, I think that changing it by one able to support higher heat is useless, because we saw during all our experiment that the temperature never approaches the 598 K TEG threshold.

In my opinion, while waiting for some more improvements of the TEG properties, the best way to recover more energy is to increase the temperature gradient. To do so we can either try to increase the hot surface temperature or to decrease the cold surface one.

The hot surface temperature depends on the amount of heat going through the pad. The only two ways to increase this amount of heat would be to put the TEG closer to the friction surface or to use a metal with an thermal conductivity higher than the copper. The first option was not recommended after the the modeling analysis to avoid to reach the TEG temperature threshold, but after considering our experimental results, I think that it would be interesting investigate since the temperature picked up are far away from this threshold. Using another metal with an higher heat conductivity than the copper as heat source is not an option, indeed only very expensive metal have such characteristics. Using them as the copper to replace a part of the friction surface would therefore be impossible.

Decreasing the hot surface temperature would be a good way to investigate, we could for example try some other metal, even if the modeling analysis shown us than iron was the most efficient one. Another way would be to use a cooling system, but the dimension, the cost and the energy consumption of such systems is not adapted to our problematic. Our last option would be to put the TEG cold surface in contact with the air. This would allow the cold surface to remain way cooler than it does with our setup. We could for example manufactured the brake pad to allow an air flux to reach the cold surface and have some air convection.

But even with all this improvements, it is hard to think that the amount of energy recovered would be interesting for a middle range car. Indeed a car need around 2kW of electricity to power its electrical components. Our production seems then way to low to be used on a car. But as presented in the introduction, this concept was not investigated to be used on cars but on heavy vehicles as trucks, trains or metros. That makes no doubts that the amount of energy energy available for recovery in this vehicles is more important. Furthermore the dimensions of the TEG could be bigger and the recovery more important.

Even if our experiments shown us that the efficiency of our concept is low if adapted on a car, we have to think that it is an easy, light and cheap way to slightly decrease the energy consumption which may deserve to be investigating on heavy vehicles.

Bibliography

Congress, 2012. Green car congress 2011 URL
http://www.greencarcongress.com/2011/11/dotepa-20111116.html#more

Montgomery, 2005. Douglas C Montgomery, Design and Analysis of Experiment 6th edition, WILEY 2005.

Rosendahl, Mortensen, og Enkeshafi, 2011. Lasse A. Rosendahl, Paw V. Mortensen, og Ali Enkeshafi, 2011. Joint presentation at 30th international conference on thermoelectrics.

Plouchard, 2004. Georgia Plouchart, La consommation 'énergie dans le domaine des transports, IFP, december 2004.

Stockohlm,2002. J. G. Stockholm, Energie portable : autonomie et intégration dans l'environnement humain. mars 2002, Journées Electrotechniques du Club EEA.

Syrota 2008. J Syrota, Rapport Mission "vehicule 2030" septembre 2008.

Techniques de l'ingénieur, 2012. URL
http://www.techniques-ingenieur.fr/energies-th4/reseaux-electriques-de-transport-et-de-repartition-42263210/stockage-inertiel-de-l-energie-d4030/volant-d-inertie-d4030v2niv10002.html

TEGPower.com.
http://www.tegpower.com/

8 Appendix

Appendix 8.1 Radial heat profile experiment

Results obtained for the four experiments

	brake pad high (mm)			
time (s)	15	30	45	60
2	296,739	296,768	296,845	297,306
4	297,656	298,236	298,133	299,761
6	298,675	299,748	299,922	300,993
8	299,946	301,046	301,648	301,697
10	301,428	301,979	302,276	303,889
12	303,346	302,429	304,869	304,825
14	304,186	303,371	305,25	306,665
16	305,538	304,179	307,238	308,049
18	306,995	306,559	308,909	309,985
20	307,138	307,962	309,376	310,056
22	308,218	309,039	310,835	311,208
24	309,346	311,193	311,688	311,924
26	310,642	311,892	312,177	313,783
28	310,929	312,457	313,546	314,208
30	311,506	313,291	313,933	314,949
2	297,154	297,742	298,059	298,081
4	298,196	298,758	300,269	300,304
6	298,579	300,033	302,558	302,953
8	299,26	301,591	303,11	304,304
10	345,039	302,212	303,388	305,725
12	301,963	303,083	305,165	306,438
14	302,314	305,678	306,548	306,633
16	303,356	306,164	307,302	307,602
18	304,378	306,434	308,26	308,393
20	305,124	307,084	308,716	308,721
22	305,899	308,248	308,959	309,208
24	306,399	308,906	309,219	310,176
26	306,982	309,096	310,219	311,208
28	307,643	309,568	310,558	311,964
30	308,675	310,282	311,75	312,496
2	296,186	296,611	297,644	299,304
4	297,174	297,944	299,26	300,696
6	298,931	298,656	299,857	302,592
8	300,208	300,309	302,771	303,017
10	301,453	302,654	303,146	304,876
12	281,707	303,484	304,771	305,985
14	303,707	304,741	306,58	307,113
16	304,599	305,557	307,196	308,857
18	304,995	306,483	308,037	309,285
20	305,186	306,695	309,146	309,538
22	306,004	307,125	309,619	310,697
24	306,973	307,911	310,452	311,378
26	307,516	308,995	311,228	311,633
28	308,152	309,326	311,781	312,697
30	308,665	310,483	311,909	313,925
2	297,154	298,579	297,356	300,24
4	298,55	298,785	299,931	300,976
6	299,163	299,196	302,602	302,113
8	299,413	301,331	284,155	303,304
10	300,963	302,511	304,867	305,432
12	300,41	303,196	305,388	306,368
14	301,57	305,827	306,253	307,368
16	304,314	305,899	306,282	308,336
18	305,027	306,685	306,707	308,996
20	305,899	306,83	307,299	309,368
22	307,876	307,186	309,133	310,113
24	308,803	307,485	309,047	311,049
26	308,685	308,188	309,813	311,113
28	309,132	309,311	310,653	312,049
30	309,602	309,966	310,919	312,921

All the results in the yellow cases are out of range and are then not used in the average values calculating

Average values of the temperatures

		brake pad high (mm)			
		15	30	45	60
time (s)	2	296,81	297,43	297,48	298,73
	4	297,89	298,43	299,40	300,43
	6	298,84	299,41	301,23	302,16
	8	299,71	301,07	302,51	303,08
	10	301,28	302,34	303,42	304,98
	12	301,91	303,05	305,05	305,90
	14	302,94	304,90	306,16	306,94
	16	304,45	305,45	307,00	308,21
	18	305,35	306,54	307,98	309,16
	20	305,84	307,14	308,63	309,42
	22	307,00	307,90	309,64	310,31
	24	307,88	308,87	310,10	311,13
	26	308,46	309,54	310,86	311,93
	28	308,96	310,17	311,63	312,73
	30	309,61	311,01	312,13	313,57

Radial heat profile

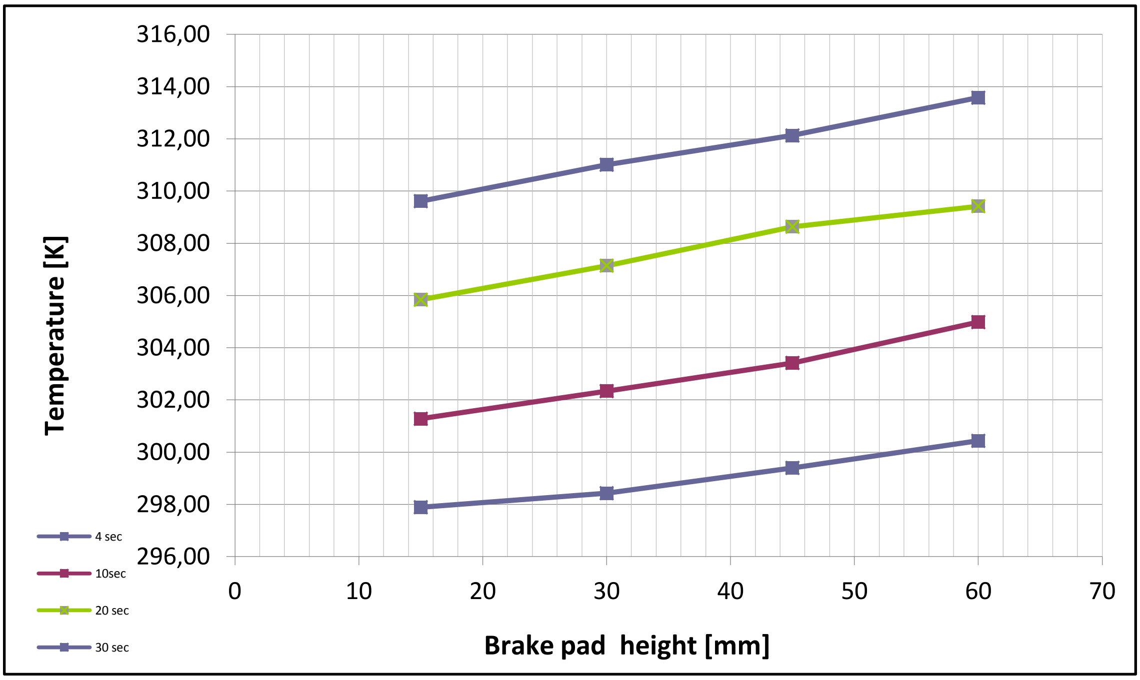

Appendix 8.2 Azimuthal heat profile experiment

Results obtained for the four experiments

		brake pad high (mm)				
		18	36	54	72	90
time (s)	2	297,462	296,852	296,916	297,579	296,477
	4	297,695	297,98	298,004	297,331	297,334
	6	298,921	299,108	299,044	298,992	297,307
	8	299,665	299,044	299,788	300,43	299,799
	10	300,643	300,788	300,012	301,663	300,693
	12	300,982	301,172	301,268	301,29	300,373
	14	301,749	302,012	302,948	303,194	302,555
	16	301,633	304,363	303,874	304,599	303,354
	18	302,95	304,948	304,066	305,96	304,194
	20	304,641	306,756	306,268	306,088	305,715
	22	306,312	308,012	305,299	307,715	306,459
	24	307,346	309,172	307,268	308,447	306,97
	26	309,739	309,948	308,076	310,277	308,821
	28	310,653	310,236	308,81	310,896	309,629
	30	312,4	310,044	310,417	311,014	310,681
	2	298,464	298,236	297,619	298,803	297,776
	4	299,761	298,788	297,416	299,4	297,978
	6	300,336	299,14	298,651	299,941	298,946
	8	300,579	301,108	298,788	300,312	299,627
	10	301,027	302,204	299,788	301,759	299,978
	12	302,122	303,948	301,884	303,611	301,042
	14	303,801	304,076	302,172	304,066	302,371
	16	304,921	304,268	303,948	304,132	304,233
	18	305,189	306,363	303,948	305,068	305,671
	20	305,845	306,884	304,756	305,685	306,204
	22	306,226	307,044	306,236	306,12	306,459
	24	308,538	308,108	308,268	308,292	307,843
	26	309,663	309,204	310,916	308,845	308,45
	28	311,471	310,363	311,572	309,631	309,513
	30	312,577	311,98	312,212	310,814	311,747
	2	296,044	296,612	296,936	295,931	295,769
	4	297,931	297,331	297,548	296,056	296,958
	6	298,889	297,268	298,98	298,788	298,086
	8	300,093	298,459	300,012	299,449	299,383
	10	302,061	299,948	300,788	300,688	300,319
	12	303,985	301,012	301,012	300,442	301,511
	14	304,739	301,98	302,172	301,889	302,106
	16	305,336	303,395	302,916	303,027	303,649
	18	306,135	303,948	304,363	303,815	303,872
	20	307,43	304,916	305,044	304,911	303,457
	22	307,206	305,82	306,044	305,579	305,808
	24	308,12	307,044	307,14	307,439	307,415
	26	309,538	309,108	308,948	309,683	308,447
	28	310,358	310,608	310,82	310,57	309,629
	30	311,707	312,044	312,24	311,538	311,587
	2	298,294	298,48	299,572	299,113	297,96
	4	299,022	299,853	300,176	299,697	299,333
	6	300,744	301,476	300,732	300,304	300,681
	8	301,906	302,412	301,668	301,746	301,125
	10	302,331	302,412	302,859	302,297	302,371
	12	307,395	303,157	302,604	303,523	302,744
	14	304,52	304,157	303,348	304,948	303,754
	16	305,139	305,348	305,348	305,022	303,116
	18	305,127	306,412	306,859	306,722	305,445
	20	306,223	308,572	307,732	308,019	306,838
	22	308,415	308,253	309,476	308,616	307,87
	24	309,533	309,476	310,54	309,53	308,966
	26	310,299	310,157	311,019	310,353	310,307
	28	311,978	311,348	312,412	311,213	311,604
	30	313,267	312,125	313,636	312,238	312,106

Average values of the temperatures

	brake pad high (mm)				
time (s)	18	36	54	72	90
2	297,57	297,55	297,76	297,86	297,00
4	298,60	298,49	298,29	298,12	297,90
6	299,72	299,25	299,35	299,51	298,76
8	300,56	300,26	299,53	300,48	299,98
10	301,68	301,34	300,86	301,60	300,84
12	303,50	302,32	301,69	302,22	301,42
14	303,70	303,06	302,66	303,52	302,70
16	304,26	304,34	304,02	304,20	303,59
18	304,85	305,42	304,81	305,39	304,80
20	306,03	306,78	305,95	306,18	305,55
22	307,04	307,28	306,76	307,01	306,65
24	308,38	308,45	308,30	308,43	307,80
26	309,81	309,60	309,74	309,79	309,01
28	311,12	310,64	310,90	310,58	310,09
30	312,49	311,55	312,13	311,40	311,53

Azimuthal heat profile

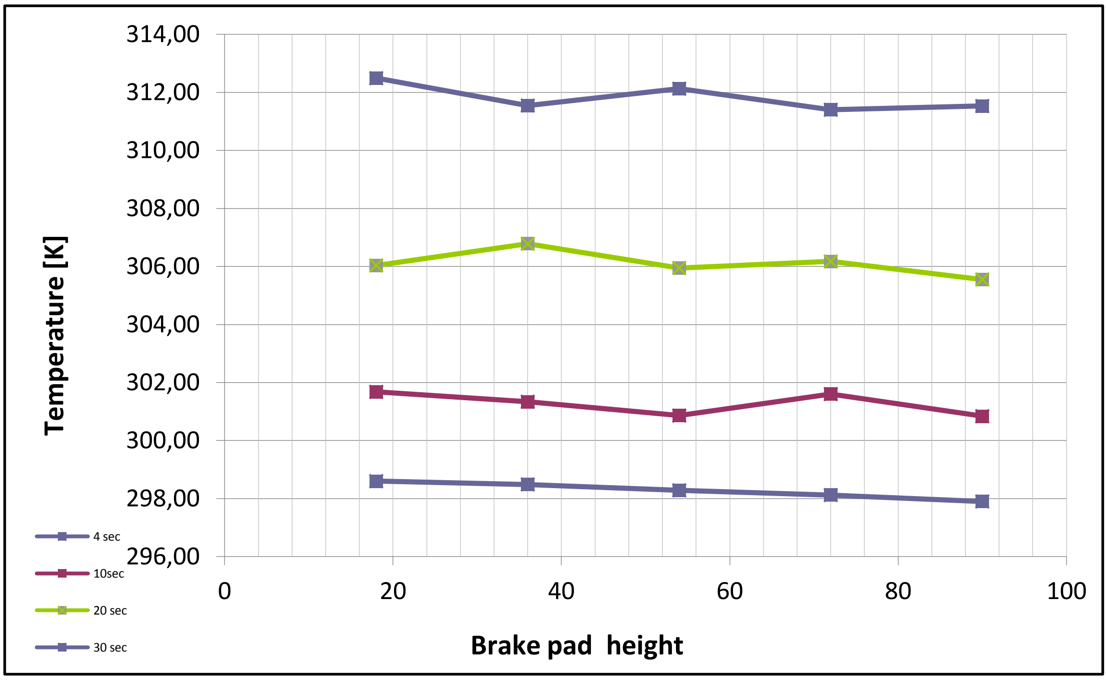

Appendix 8.3 Thicknessl heat profile experiment using an unmodified brake pac

Results obtained during the four experiments

	brake pad thickness (mm)							
time (s)	2	4	6	8	10	12	14	16
2	297,562	296,917	296,779	296,497	297,006	297,179	296,868	296,857
4	297,695	298,004	297,656	297,334	297,761	297,331	297,236	296,98
6	298,921	299,044	298,675	297,307	296,993	297,692	297,448	297,108
8	300,665	299,85	298,946	297,799	297,697	297,43	297,046	297,044
10	302,643	300,012	298,828	298,693	297,889	297,663	296,979	297,088
12	302,982	301,488	299,346	298,973	297,825	297,29	297,429	297,172
14	303,749	302,948	300,186	299,555	298,665	297,194	297,371	297,012
16	305,633	303,874	301,538	299,354	298,049	297,599	297,179	297,363
18	306,95	304,066	302,995	300,194	298,985	297,96	297,559	296,848
20	308,641	305,568	303,238	300,055	299,056	298,088	297,962	297,356
22	309,312	307,299	304,218	301,659	299,208	298,715	298,039	297,012
24	311,346	308,268	304,946	301,97	299,924	299,447	298,193	297,172
26	313,739	309,076	305,642	302,821	300,783	299,277	298,892	297,548
28	314,653	311,81	305,929	303,629	301,208	299,896	298,457	297,236
30	316,8	312,417	306,506	303,681	301,349	300,014	298,291	297,044
2	298,164	297,619	297,154	297,776	297,081	296,803	297,742	297,236
4	299,761	297,416	298,196	297,978	297,304	296,74	296,758	296,788
6	300,336	298,651	298,579	298,346	297,953	296,941	297,033	297,14
8	301,579	299,788	299,26	298,627	298,304	297,312	297,591	297,108
10	303,027	301,288	300,039	299,178	298,725	297,759	297,212	297,204
12	304,122	302,884	301,963	300,242	299,438	297,611	297,083	296,948
14	305,801	304,172	302,314	300,371	299,633	298,066	297,678	297,076
16	306,921	304,948	302,356	300,833	299,602	298,132	297,164	297,268
18	307,989	305,948	302,678	301,271	300,393	299,068	298,434	297,363
20	310,845	306,056	303,024	301,304	300,221	299,685	298,084	296,884
22	311,226	308,236	303,769	302,559	300,208	299,712	298,248	297,044
24	312,538	309,268	304,199	302,243	301,176	300,292	298,906	297,108
26	313,663	310,916	304,982	302,85	301,208	300,845	299,096	297,204
28	315,471	311,572	305,643	303,513	301,364	300,631	299,568	297,363
30	317,977	311,212	305,675	303,747	301,496	300,814	299,282	297,98
2	296,744	296,936	296,186	295,769	298,304	295,931	296,611	296,612
4	298,731	297,548	297,174	296,158	296,696	296,456	296,144	296,331
6	300,889	298,98	298,931	296,086	296,592	296,788	296,656	296,268
8	301,893	300,012	299,208	297,383	297,217	297,449	296,309	296,459
10	304,061	301,788	300,253	297,319	297,876	297,688	296,654	296,248
12	306,985	303,512	301,187	298,011	297,985	297,442	297,484	296,012
14	307,439	305,172	301,707	299,106	298,113	297,889	297,741	296,48
16	309,336	305,916	302,599	299,649	298,857	298,027	297,557	296,395
18	310,135	306,363	303,995	299,872	298,285	298,215	297,483	296,948
20	312,43	306,444	303,186	299,957	298,538	298,911	297,695	296,916
22	312,806	307,074	303,604	301,608	299,697	298,579	297,125	296,82
24	313,12	308,14	304,973	301,815	300,378	299,439	297,911	297,044
26	315,538	309,548	305,516	302,447	300,633	299,683	297,995	296,108
28	316,358	310,22	306,152	302,629	301,297	299,57	298,326	296,608
30	317,707	311,24	306,365	302,887	301,225	299,538	298,483	296,844
2	297,294	297,572	297,154	297,06	296,24	296,113	296,579	296,48
4	299,022	298,176	297,55	297,333	296,976	296,697	296,785	296,853
6	300,744	299,732	298,163	298,181	296,413	296,304	296,796	297,476
8	301,906	301,668	298,618	298,125	297,004	296,746	297,331	297,412
10	302,931	301,459	299,763	298,55	297,432	297,297	297,111	297,412
12	303,395	302,604	300,41	298,744	298,368	297,523	297,196	296,857
14	305,52	303,348	301,57	299,754	298,368	297,948	297,827	297,157
16	307,139	305,393	301,765	300,116	299,336	298,022	297,899	297,348
18	308,627	306,859	302,027	300,445	299,996	298,722	297,685	297,412
20	310,223	306,738	302,399	300,538	300,368	298,819	297,83	297,572
22	310,415	307,478	303,276	301,87	300,813	298,916	298,186	297,253
24	312,533	308,54	304,556	301,966	301,049	299,53	298,485	297,476
26	314,299	310,019	305,085	302,307	301,113	299,353	298,188	297,457
28	315,978	310,475	305,632	302,604	301,049	299,213	298,311	297,648
30	317,267	311,637	306,002	303,106	301,221	299,238	298,466	297,825

Average values of the temperatures

time (s)	brake pad thickness (mm) 2,0	4,0	6,0	8,0	10,0	12,0	14,0	16,0
2	297,4	297,3	296,8	296,8	297,2	296,5	297,0	296,8
4	298,8	297,8	297,6	297,2	297,2	296,8	296,7	296,7
6	300,2	299,1	298,6	297,5	297,0	296,9	297,0	297,0
8	301,5	300,3	299,0	298,0	297,6	297,2	297,1	297,0
10	303,2	301,1	299,7	298,4	298,0	297,6	297,0	297,0
12	304,4	302,6	300,7	299,0	298,4	297,5	297,3	296,7
14	305,6	303,9	301,4	299,7	298,7	297,8	297,7	296,9
16	307,3	305,0	302,1	300,0	299,0	297,9	297,4	297,1
18	308,4	305,8	302,9	300,4	299,4	298,5	297,8	297,1
20	310,5	306,2	303,0	300,5	299,5	298,9	297,9	297,2
22	310,9	307,5	303,7	301,9	300,0	299,0	297,9	297,0
24	312,4	308,6	304,7	302,0	300,6	299,7	298,4	297,2
26	314,3	309,9	305,3	302,6	300,9	299,8	298,5	297,1
28	315,6	311,0	305,8	303,1	301,2	299,8	298,7	297,2
30	317,4	311,6	306,1	303,4	301,3	299,9	298,6	297,4

Temperature profile

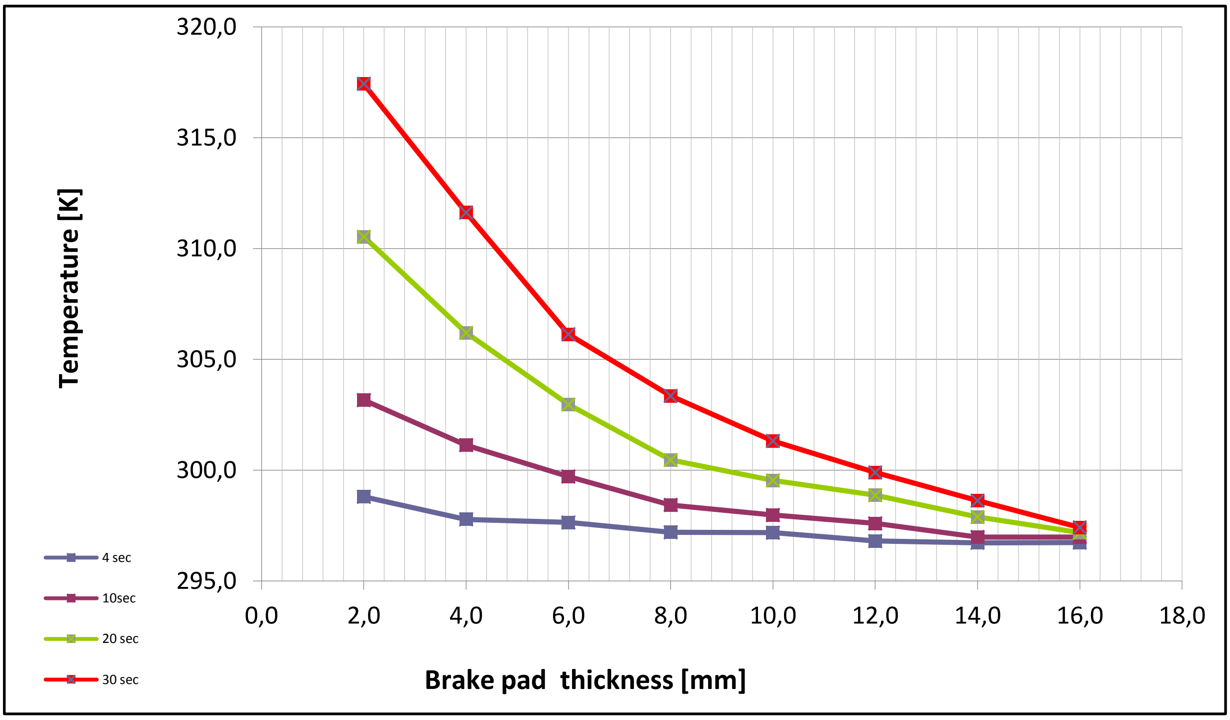

Appendix 8.4 Thickness heat profile experiment using a copper heat source

Results obtained during the four experiments

		brake pad thickness (mm)							
		2	4	6	8	10	12	14	16
time (s)	2	299,368	298,631	296,823	295,673	296,024	297,036	296,474	297,334
	4	305,027	303,567	296,823	296,513	296,024	297,068	297,41	296,024
	6	310,371	317,887	297,231	297,545	296,769	297,264	297,017	296,152
	8	315,594	313,695	298,759	299,641	297,896	297,605	297,761	296,805
	10	322,604	319,695	299,759	301,609	298,769	297,836	298,314	297,366
	12	329,294	325,791	303,919	301,456	299,992	298,081	298,378	297,302
	14	339,665	332,887	307,791	302,29	300,641	298,909	298,506	297,878
	16	349,176	338,727	312,759	303,577	301,705	299,417	299,378	298,346
	18	345,771	344,078	315,695	305,609	302,833	299,909	299,506	298,941
	20	353,41	349,535	317,567	306,865	303,737	300,909	299,442	299,081
	22	356,737	353,791	320,727	308,609	306,024	301,1	299,538	299,254
	24	360,019	357,535	323,95	310,513	305,577	301,973	299,825	298,42
	26	366,122	361,727	326,11	312,545	306,801	302,685	299,985	299,506
	28	371,221	365,663	328,982	315,417	308,673	303,845	300,113	299,889
	30	377,717	368,855	331,046	317,513	309,801	304,653	299,761	300,688
	2	299,385	299,046	297,142	295,905	295,737	297,121	296,633	296,727
	4	304,982	302,919	296,919	296,745	296,645	297,077	296,25	296,324
	6	312,027	310,695	298,759	298,449	297,801	297,609	297,889	296,887
	8	317,611	316,855	300,663	300,226	298,533	297,941	296,697	297,366
	10	324,42	321,823	304,567	301,705	299,337	298,336	297,697	297,452
	12	332,439	326,919	309,823	302,449	299,992	298,85	297,921	297,887
	14	340,208	331,982	312,663	303,737	300,205	299,1	297,665	297,248
	16	348,548	337,855	316,919	306,449	300,641	300,005	298,506	298,09
	18	354,548	341,887	319,855	308,545	301,705	300,877	299,049	297,909
	20	360,896	349,567	321,791	310,801	301,992	301,845	299,538	298,995
	22	364,017	353,611	324,95	313,737	302,896	302,781	299,985	298,911
	24	368,931	357,567	327,727	314,705	304,024	302,973	299,633	299,262
	26	371,751	360,312	330,791	316,673	305,641	303,132	300,145	298,456
	28	376,508	364,439	332,254	319,769	307,609	304,1	300,113	299,729
	30	379,059	369,727	335,919	321,481	308,801	305,909	300,825	299,506
	2	300,316	299,759	296,823	296,705	296,641	297,277	295,825	295,921
	4	305,176	302,823	296,919	296,641	296,705	297,073	296,161	295,872
	6	311,894	309,535	297,759	297,641	297,928	297,373	296,41	296,727
	8	318,636	316,599	299,887	298,577	298,737	297,609	296,793	296,976
	10	325,073	322,567	304,727	299,577	299,388	298,045	297,761	297,899
	12	330,913	328,631	308,567	301,481	300,833	298,973	297,857	298,466
	14	337,147	334,663	311,695	302,737	301,96	299,036	298,538	298,326
	16	343,046	339,471	314,791	303,226	302,928	299,685	299,825	298,2
	18	347,366	342,631	317,791	304,577	303,609	300,717	299,665	299,071
	20	350,631	345,855	320,046	305,801	303,705	301,621	299,857	299,304
	22	355,24	349,823	321,078	308,353	304,769	302,749	299,538	295,299
	24	362,452	350,759	323,297	310,705	305,545	303,005	300,538	298,516
	26	369,103	355,599	325,919	312,385	306,184	303,845	300,602	300,24
	28	375,764	360,791	329,823	315,417	306,769	304,036	300,985	300,938
	30	381,294	367,95	329,791	317,417	309,769	305,068	301,665	300,272
	2	299,113	299,471	297,174	296,705	296,469	295,557	296,602	296,132
	4	304,061	302,174	296,823	296,545	296,769	296,785	296,665	296,867
	6	310,761	308,855	298,695	297,322	297,577	297,673	296,857	297,675
	8	318,049	315,727	300,823	299,258	297,801	296,813	297,186	297,41
	10	326,24	321,855	302,759	300,481	298,801	297,209	297,793	297,508
	12	335,049	330,663	305,046	302,513	299,205	298,941	298,017	297,231
	14	341,009	335,887	307,95	302,673	299,96	298,813	298,857	298,56
	16	348,56	339,823	311,791	304,449	301,056	299,132	299,314	299,985
	18	354,346	342,663	314,174	306,673	301,513	300,653	299,017	299,761
	20	359,24	346,663	318,334	308,385	302,96	301,781	299,633	298,503
	22	364,068	350,599	320,695	310,801	303,896	302,1	299,793	298,007
	24	368,206	357,855	324,462	312,577	305,12	303,445	299,41	298,346
	26	372,186	362,631	329,727	315,545	306,609	304,973	299,921	298,837
	28	379,122	366,663	331,95	317,353	308,96	305,1	300,538	298,005
	30	383,759	371,791	335,014	320,545	310,833	306,341	301,506	299,506

Average values of the temperatures

		brake pad thickness (mm)							
		2,0	4,0	6,0	8,0	10,0	12,0	14,0	16,0
time (s)	2	299,5	299,2	297,0	296,2	296,2	296,7	296,4	296,5
	4	304,8	302,9	296,9	296,6	296,5	297,0	296,6	296,3
	6	311,3	311,7	298,1	297,7	297,5	297,5	297,0	296,9
	8	317,5	315,7	300,0	299,4	298,2	297,5	297,1	297,1
	10	324,6	321,5	303,0	300,8	299,1	297,9	297,9	297,6
	12	331,9	328,0	306,8	302,0	300,0	298,7	298,0	297,7
	14	339,5	333,9	310,0	302,9	300,7	299,0	298,4	298,0
	16	347,3	339,0	314,1	304,4	301,6	299,6	299,3	298,7
	18	350,5	342,8	316,9	306,4	302,4	300,5	299,3	298,9
	20	356,0	347,9	319,4	308,0	303,1	301,5	299,6	299,0
	22	360,0	352,0	321,9	310,4	304,4	302,2	299,7	297,9
	24	364,9	355,9	324,9	312,1	305,1	302,8	299,9	298,6
	26	369,8	360,1	328,1	314,3	306,3	303,7	300,2	299,3
	28	375,7	364,4	330,8	317,0	308,0	304,3	300,4	299,6
	30	380,5	369,6	332,9	319,2	309,8	305,5	300,9	300,0

Temperature profile

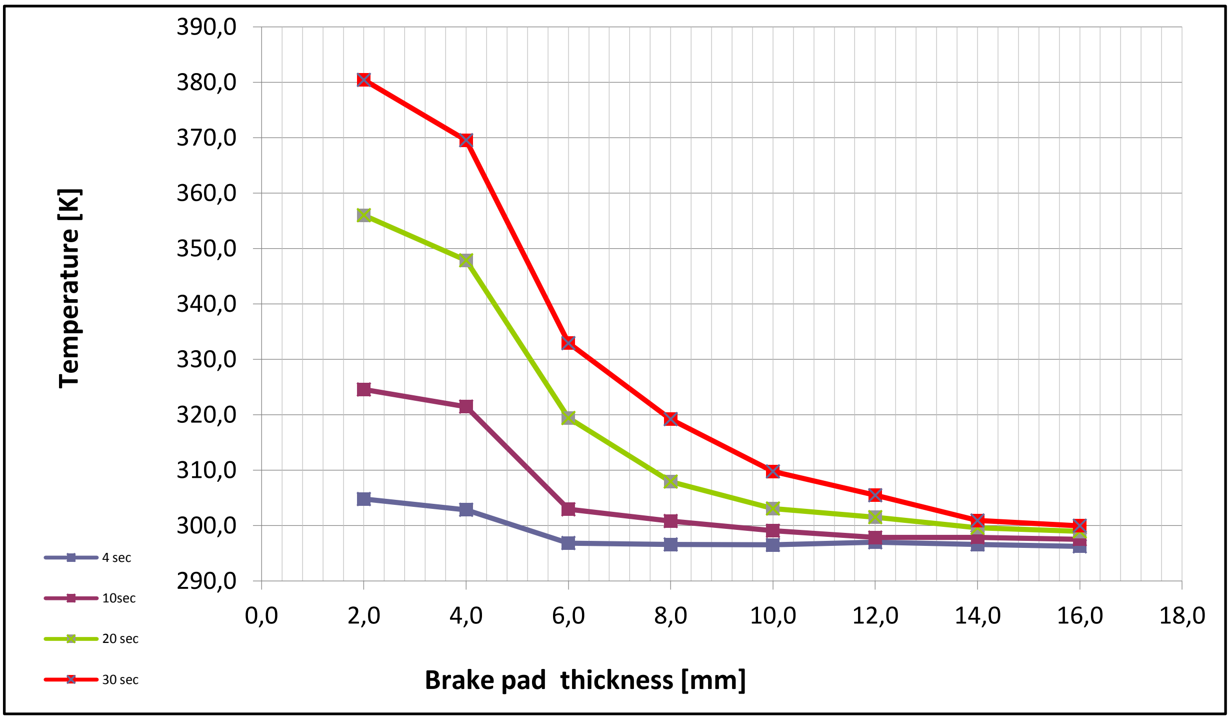

Appendix 8.5 Thickness heat profile experiment using a copper heat source and the TEG

Results obtained during the four experiments

	brake pad thickness (mm)						
time (s)	2	4	8	10	12	14	16
2	298,368	297,631	295,873	296,224	296,136	296,474	296,334
4	301,27	299,567	296,213	296,024	296,068	296,41	296,024
6	303,371	302,887	298,545	296,769	296,164	296,017	296,152
8	307,594	305,695	299,641	297,896	296,505	296,761	296,805
10	315,604	310,695	301,609	298,769	297,036	296,714	297,366
12	325,294	316,791	304,577	299,992	297,781	297,378	297,302
14	332,665	323,887	307,29	301,641	298,909	297,506	297,078
16	339,176	328,727	313,577	303,705	298,717	298,378	298,346
18	345,771	334,078	316,609	305,833	299,909	299,506	299,941
20	351,41	340,535	321,865	306,737	300,909	299,642	300,081
22	360,737	345,791	326,609	308,024	303,1	300,538	301,646
24	368,019	349,535	327,513	311,577	304,973	302,825	301,42
26	373,122	355,727	333,545	313,801	306,685	304,985	302,506
28	375,221	360,663	338,417	315,673	308,845	306,113	302,889
30	377,717	365,855	343,513	317,801	311,653	307,761	305,688
2	298,385	297,046	296,205	295,737	295,821	296,133	296,727
4	300,982	297,919	296,545	295,945	295,877	296,25	296,324
6	304,027	300,695	297,449	296,301	296,209	296,889	296,887
8	313,611	305,855	298,226	296,833	296,441	296,697	297,366
10	321,42	310,823	300,705	297,737	297,036	297,697	298,452
12	330,439	317,919	302,449	298,992	297,32	297,921	296,887
14	336,208	321,982	306,737	299,705	298,1	298,665	296,248
16	342,548	325,855	309,449	301,641	299,005	299,506	299,09
18	347,867	330,887	312,545	303,705	300,877	300,049	297,909
20	352,896	337,567	317,801	305,992	302,845	299,538	298,995
22	357,017	343,611	321,737	308,896	305,781	300,985	300,911
24	361,931	348,567	327,705	310,024	306,973	301,633	301,262
26	366,751	354,312	333,673	313,641	309,132	303,145	304,456
28	371,508	360,439	338,769	315,609	311,1	305,113	306,729
30	376,059	366,127	343,481	316,801	313,909	308,825	308,506
2	297,316	296,759	295,705	295,641	295,877	295,825	295,921
4	300,176	298,823	296,241	295,705	295,973	295,761	295,872
6	305,894	301,535	297,641	295,928	296,173	296,41	296,727
8	315,636	306,599	299,577	296,737	297,409	296,793	296,376
10	322,073	313,567	302,577	297,088	297,845	296,761	297,899
12	329,913	317,631	305,481	298,833	297,973	297,857	297,466
14	335,147	323,663	311,737	299,96	298,436	297,538	297,326
16	341,046	330,471	315,226	301,523	299,685	298,825	298,592
18	348,366	336,631	318,577	303,609	300,717	299,665	299,071
20	353,631	341,855	320,801	305,705	301,621	299,857	299,304
22	358,24	345,823	324,353	308,769	303,749	300,538	300,449
24	364,452	350,759	329,705	311,545	306,254	301,538	301,516
26	369,103	356,599	334,385	313,184	308,845	303,602	302,24
28	374,764	361,791	338,417	316,769	310,036	305,985	305,938
30	376,294	366,45	343,417	318,769	313,068	307,665	307,272
2	298,113	296,471	296,705	296,769	296,557	296,602	296,132
4	302,061	297,774	296,845	296,769	296,685	296,665	296,867
6	304,761	301,855	297,322	297,077	297,173	296,857	296,675
8	313,049	307,727	299,258	297,801	297,413	297,186	297,01
10	322,24	312,855	302,481	298,801	297,909	297,793	297,508
12	331,049	317,663	305,213	298,705	298,641	298,017	298,231
14	338,009	326,887	311,673	299,96	299,613	298,857	298,56
16	344,56	332,823	315,449	300,056	299,632	299,314	298,985
18	349,346	338,663	319,673	303,513	300,653	300,017	299,261
20	353,24	343,663	323,385	304,96	302,781	301,633	299,503
22	359,068	350,599	328,801	308,296	305,1	302,793	301,007
24	365,206	356,855	332,577	310,12	308,845	304,41	303,346
26	370,186	361,631	336,545	312,609	311,973	306,25	305,837
28	375,122	364,663	340,353	315,96	313,1	305,538	306,005
30	377,759	367,491	344,545	319,833	314,005	309,95	308,506

Average values of the temperatures

		brake pad thickness (mm)						
		2,0	4,0	8,0	10,0	12,0	14,0	16,0
time (s)	2	298,0	297,0	296,1	296,1	296,1	296,3	296,3
	4	301,1	298,5	296,5	296,1	296,2	296,3	296,3
	6	304,5	301,7	297,7	296,5	296,4	296,5	296,6
	8	312,5	306,5	299,2	297,3	296,9	296,9	296,9
	10	320,3	312,0	301,8	298,1	297,5	297,2	297,8
	12	329,2	317,5	304,4	299,1	297,9	297,8	297,5
	14	335,5	324,1	309,4	300,3	298,8	298,1	297,3
	16	341,8	329,5	313,4	301,7	299,3	299,0	298,8
	18	347,8	335,1	316,9	304,2	300,5	299,8	299,0
	20	352,8	340,9	321,0	305,8	302,0	300,2	299,5
	22	358,8	346,5	325,4	308,5	304,4	301,2	301,0
	24	364,9	351,4	329,4	310,8	306,8	302,6	301,9
	26	369,8	357,1	334,5	313,3	309,2	304,5	303,8
	28	374,2	361,9	339,0	316,0	310,8	305,7	305,4
	30	377,0	366,5	343,7	318,3	313,2	308,6	307,5

Temperature profile

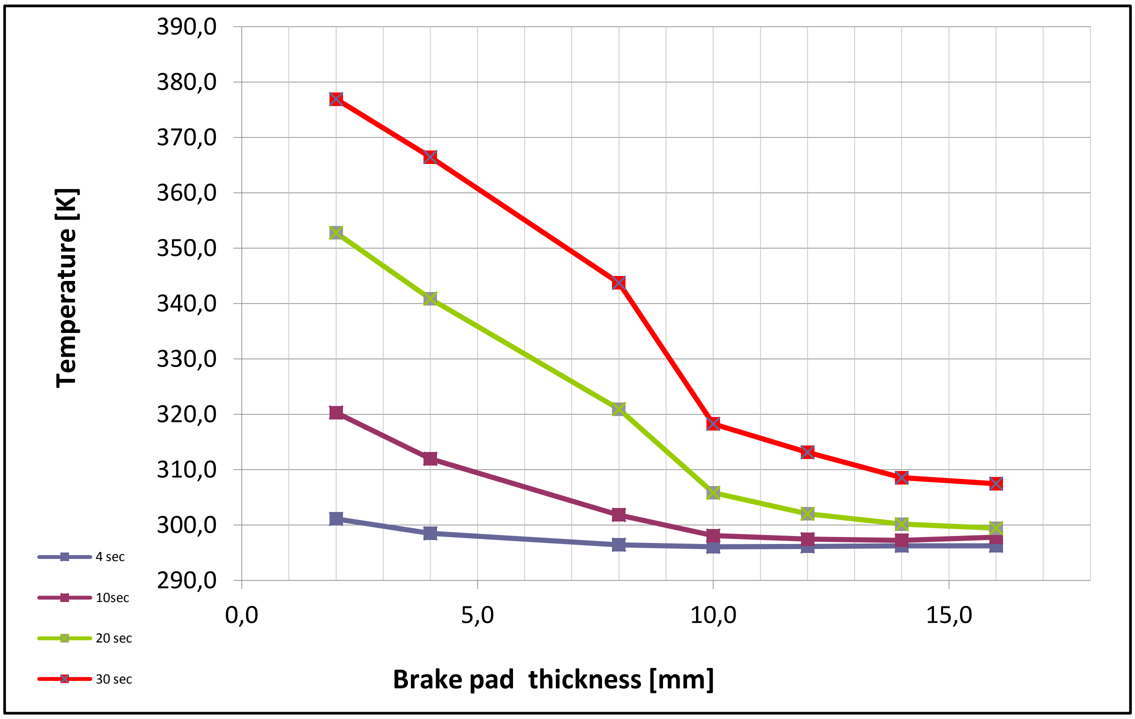

Appendix 8.6 Thickness heat profile experiment using a copper heat source, the TEG and an iron heat sink

Results obtained during the four experiments

	brake pad thickness (mm)						
time (s)	2	4	8	10	12	14	16
2	298,89	296,874	296,152	296,191	295,562	295,353	295,97
4	301,721	298,368	297,328	296,744	295,899	295,513	295,734
6	304,094	301,888	299,125	297,734	296,522	295,905	295,874
8	312,839	305,862	301,351	298,193	298,034	297,769	296,406
10	318,637	311,58	304,32	300,021	299,542	298,609	296,833
12	325,46	315,618	306,331	301,078	300,93	298,905	297,162
14	331,013	318,52	309,684	303,697	302,78	299,874	298,194
16	334,586	321,478	311,058	304,834	303,92	301,97	299,002
18	338,991	327,999	316,738	306,1	305,707	304,619	300,842
20	341,345	332,672	317,822	309,161	310,002	307,427	303,13
22	349,959	338,594	319,918	313,653	313,279	309,427	304,13
24	354,716	345,979	321,694	316,662	315,014	311,842	307,715
26	361,46	351,385	325,439	318,535	318,618	313,81	309,162
28	369,642	357,864	331,407	324,225	320,459	314,779	311,938
30	374,229	362,517	336,245	326,181	321,758	315,938	312,747
2	297,526	297,026	296,456	296,099	296,542	295,683	295,906
4	299,497	299,748	297,456	296,842	296,638	295,983	296,034
6	303,168	302,589	298,727	298,179	297,211	296,13	296,779
8	309,635	309,992	300,498	299,69	298,849	297,13	296,81
10	316,932	316,142	303,267	301,127	299,527	298,766	297,906
12	322,026	321,918	305,095	304,881	299,604	299,779	299,002
14	329,721	326,952	308,827	306,51	301,213	300,449	300,098
16	336,836	330,554	310,407	308,321	304,638	302,97	302,258
18	342,094	333,397	312,893	312,351	306,798	305,842	303,13
20	347,315	337,112	315,947	315,373	309,213	307,226	304,226
22	350,583	340,881	318,178	318,938	312,66	309,97	306,81
24	354,605	345,441	322,522	321,51	315,925	311,779	307,842
26	360,839	350,591	326,81	324,287	316,724	312,162	309,002
28	368,721	356,911	331,947	325,65	318,606	314,002	311,81
30	372,006	362,321	336,937	327,215	320,427	315,874	313,034
2	299,126	297,825	296,488	296,107	296,107	295,81	295,779
4	302,102	299,441	296,286	296,187	295,935	295,81	295,938
6	306,731	302,942	298,127	297,478	297,137	296,002	296,779
8	311,423	307,734	298,552	299,031	298,478	296,779	296,651
10	318,721	314,454	299,67	301,589	299,52	298,587	297,651
12	325,903	318,004	301,063	303,69	301,009	299,81	299,13
14	330,369	325,26	303,817	306,382	303,437	300,779	302,002
16	336,817	330,134	307,734	308,542	305,722	301,002	304,97
18	339,986	337,707	310,277	310,979	306,341	304,13	306,322
20	346,912	341,345	315,849	313,584	307,115	306,779	307,81
22	352,88	345,154	322,242	316,626	309,979	307,098	308,13
24	359,664	349,429	324,945	318,957	313,913	310,13	310,322
26	366,296	353,154	327,903	320,203	316,021	311,002	311,938
28	371,976	357,422	331,891	324,274	317,999	314,162	313,162
30	374,104	363,451	336,635	328,522	321,203	316,938	314,779
2	298,497	296,39	295,66	295,766	296,169	296,034	295,066
4	300,711	298,802	297,328	296,724	295,798	295,938	295,97
6	305,134	300,527	298,105	298,702	296,852	296,874	295,906
8	311,571	305,933	299,667	299,916	298,193	297,874	296,651
10	319,19	312,176	302,979	300,309	299,137	298,81	297,81
12	325,114	317,431	303,117	302,437	302,319	300,002	298,056
14	331,571	325,621	308,223	305,522	304,171	301,906	299,481
16	334,938	334,412	310,488	308,518	306,186	303,759	300,405
18	339,171	338,284	312,852	309,382	308,102	304,408	302,245
20	346,343	343,242	316,215	313,37	309,388	306,376	305,661
22	351,353	347,179	320,011	316,095	310,112	308,344	306,309
24	358,321	350,149	327,928	317,041	312,294	309,439	308,213
26	363,886	353,061	330,117	319,53	314,515	310,503	309,086
28	369,778	357,815	332,766	322,638	316,166	313,823	310,277
30	374,724	363,338	334,517	326,712	319,326	315,248	312,022

Average values of the temperatures

	brake pad thickness (mm)						
time (s)	2,0	4,0	8,0	10,0	12,0	14,0	16,0
2	298,5	297,0	296,2	296,0	296,1	295,7	295,7
4	301,0	299,1	297,1	296,6	296,1	295,8	295,9
6	304,8	302,0	298,5	298,0	296,9	296,2	296,3
8	311,4	307,4	300,0	299,2	298,4	297,4	296,6
10	318,4	313,6	302,6	300,8	299,4	298,7	297,6
12	324,6	318,2	303,9	303,0	301,0	299,6	298,3
14	330,7	324,1	307,6	305,5	302,9	300,8	299,9
16	335,8	329,1	309,9	307,6	305,1	302,4	301,7
18	340,1	334,3	313,2	309,7	306,7	304,7	303,1
20	345,5	338,6	316,5	312,9	308,9	307,0	305,2
22	351,2	343,0	320,1	316,3	311,5	308,7	306,3
24	356,8	347,7	324,3	318,5	314,3	310,8	308,5
26	363,1	352,0	327,6	320,6	316,5	311,9	309,8
28	370,0	357,5	332,0	324,2	318,3	314,2	311,8
30	373,8	362,9	336,1	327,2	320,7	316,0	313,1

Temperature profile

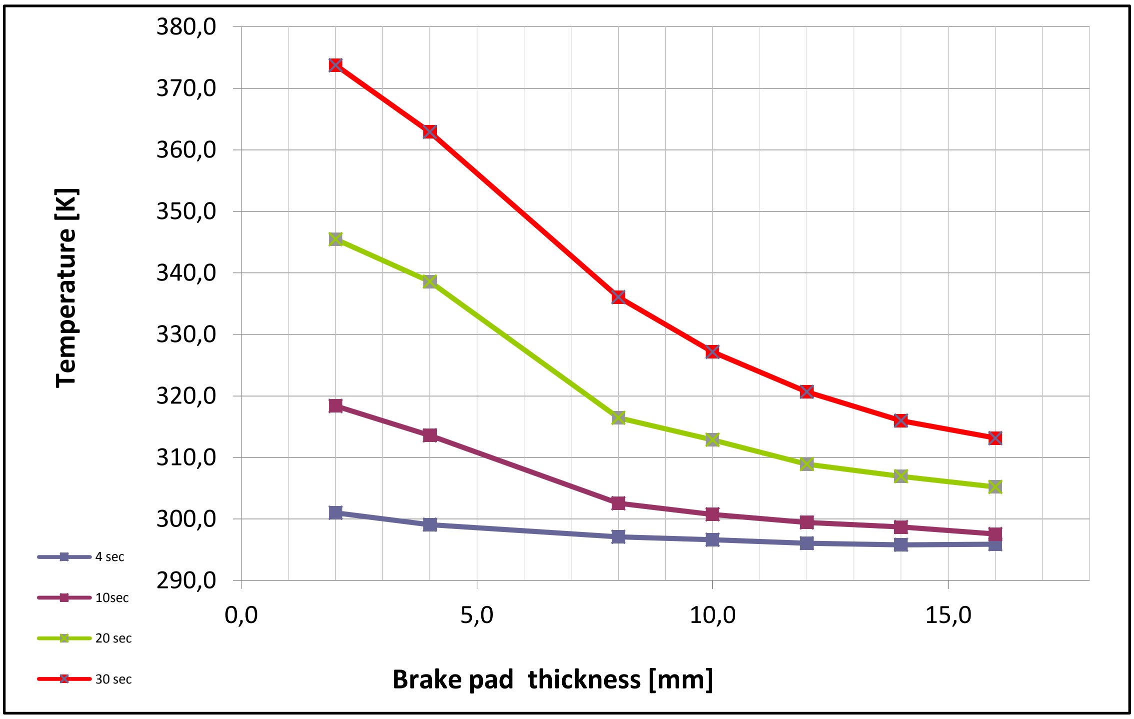

Appendix 8.7 Thickness heat profile experiment for 150 seconds

Results obtained during the four experiments

		brake pad thickness (mm)					
		2	4	8	10	12	16
time (s)	5	301,481	299,936	298,904	297,297	297,344	296,535
	10	317,108	310,572	304,747	300,916	299,238	297,344
	15	331,162	321,432	311,894	304,533	303,579	299,439
	20	342,407	331,506	318,309	309,833	310,314	302,791
	25	358,343	349,115	327,842	317,258	316,41	308,344
	30	372,619	361,783	335,81	327,695	321,017	313,408
	35	373,587	362,368	341,82	329,779	324,462	317,471
	40	373,014	363,369	344,702	334,587	327,889	322,248
	45	371,459	363,857	347,533	338,385	330,518	325,024
	50	367,682	363,346	349,459	341,088	333,174	326,088
	55	360,321	362,665	350,565	343,629	335,909	327,344
	60	356,756	360,901	351,936	344,287	337,356	328,248
	65	353,162	358,154	351,894	344,523	338,113	330,088
	70	350,577	356,931	351,034	344,172	339,158	331,584
	75	347,523	354,985	350,435	343,872	339,774	332,008
	80	345,82	352,474	349,629	343,639	338,513	332,584
	85	343,756	350,579	349,208	343,204	337,889	331,652
	90	341,095	348,631	348,734	343,044	338,282	331,408
	95	339,201	347,217	347,82	342,511	337,408	330,567
	100	338,67	345,739	346,788	340,906	336,717	329,759
	105	337,874	344,09	345,022	339,607	335,302	327,439
	110	336,331	343,068	344,586	338,812	333,931	326,152
	115	335,778	341,954	343,115	338,353	332,941	324,535
	120	333,194	340,815	340,97	337,702	332,248	323,695
	125	332,459	338,963	339,798	336,14	331,835	322,28
	130	331,353	336,007	337,725	335,341	329,408	320,749
	135	329,088	334,299	335,713	334,545	328,525	319,823
	140	327,267	332,454	334,299	333,417	328,09	318,567
	145	326,216	330,049	333,769	333,044	327,79	317,28
	150	324,503	328,4	332,747	332,277	327,165	316,312
	5	302,213	300,751	299,661	298,047	297,254	297,135
	10	318,862	310,835	305,236	301,216	299,487	297,484
	15	330,139	320,484	311,725	304,412	302,879	299,547
	20	341,034	332,717	318,213	310,833	309,614	302,652
	25	359,552	347,611	325,309	318,247	316,247	308,326
	30	372,415	361,324	333,648	326,435	321,165	313,581
	35	373,746	362,729	341,894	330,724	325,062	317,591
	40	372,884	363,602	345,255	335,759	328,109	322,324
	45	371,99	364,304	346,233	338,42	330,768	324,724
	50	369,331	363,113	348,373	341,238	332,974	326,868
	55	365,407	362,572	350,115	343,589	336,049	328,222
	60	362,714	360,624	351,67	344,315	337,246	329,212
	65	359,034	359,027	351,393	344,783	337,813	330,958
	70	356,203	357,594	351,309	344,042	338,658	331,484
	75	354,651	355,688	350,533	343,972	339,654	331,895
	80	350,012	352,518	349,927	343,689	338,433	332,384
	85	347,768	350,346	349,4	342,804	337,949	332,086
	90	343,289	347,458	348,056	342,744	337,782	331,408
	95	341,162	345,717	346,747	341,53	337,008	330,452
	100	339,299	342,941	345,213	340,646	336,685	329,679
	105	336,034	340,272	344,358	339,875	335,598	327,542
	110	335,491	338,933	342,926	338,926	334,251	325,872
	115	333,705	336,642	341,334	337,953	333,163	324,685
	120	332,565	335,64	340,215	337,002	332,388	323,356
	125	330,862	334,506	339,086	336,754	331,742	322,008
	130	329,024	332,963	337,658	335,376	329,889	320,846
	135	328,916	331,496	336,869	334,825	328,875	319,652
	140	328,395	330,036	335,42	333,681	328,054	318,566
	145	327,798	329,62	334,048	333,125	327,547	317,78
	150	326,594	328,653	332,418	332,43	326,865	316,758

time (s)	5	301,373	300,243	299,124	298,547	297,342	297,201
	10	318,449	310,682	305,357	301,357	299,263	297,362
	15	332,619	321,487	310,654	304,159	302,742	299,415
	20	342,916	332,647	319,159	310,258	309,524	302,584
	25	358,248	345,852	325,789	317,684	316,142	308,128
	30	371,493	361,824	331,648	326,369	321,362	313,695
	35	372,523	362,842	340,835	331,796	325,214	317,356
	40	371,139	361,742	344,753	335,128	328,362	322,458
	45	367,864	360,404	346,233	339,458	330,242	324,702
	50	363,449	358,113	348,373	341,394	332,845	326,846
	55	359,503	357,458	347,148	342,889	335,628	327,359
	60	356,174	356,763	348,642	344,315	337,328	328,485
	65	353,078	354,327	348,365	344,362	337,713	329,358
	70	350,162	351,547	348,024	344,025	338,658	329,584
	75	348,727	349,641	347,633	343,751	339,584	329,964
	80	346,82	347,518	346,752	343,658	338,634	330,423
	85	342,203	345,656	345,494	342,759	337,859	330,786
	90	340,948	342,458	344,056	342,152	337,582	329,608
	95	338,245	340,485	343,747	341,634	337,154	328,742
	100	337,682	338,541	342,213	340,751	335,985	327,879
	105	335,589	336,284	340,958	339,354	334,598	326,498
	110	334,768	334,915	338,926	338,658	333,781	325,898
	115	333,375	333,642	337,486	337,351	332,963	324,882
	120	331,034	332,275	337,765	337,759	332,118	323,756
	125	329,695	330,548	336,385	336,214	331,242	322,847
	130	328,599	329,813	334,258	334,376	329,259	321,821
	135	327,319	328,276	332,617	332,843	328,375	320,852
	140	325,832	327,845	331,472	331,632	327,254	319,542
	145	324,13	326,427	330,558	330,755	326,467	318,685
	150	323,375	325,648	329,452	329,159	325,753	317,254
	5	300,896	300,026	299,661	298,275	297,254	296,845
	10	316,063	310,835	305,003	301,429	299,159	297,219
	15	331,11	320,756	311,957	304,752	302,789	299,356
	20	343,714	331,845	318,754	310,369	309,369	302,842
	25	359,216	344,645	325,309	318,689	316,654	307,48
	30	371,297	358,758	331,896	324,435	321,258	313,148
	35	372,235	359,729	340,852	329,486	324,841	317,486
	40	369,852	360,604	343,369	333,499	328,356	320,862
	45	364,673	361,475	346,233	335,47	330,239	322,785
	50	360,152	360,113	348,373	338,238	332,124	324,685
	55	357,367	359,122	348,965	340,58	334,237	327,486
	60	354,844	358,224	349,658	341,215	335,246	328,486
	65	350,643	356,327	349,393	341,653	335,87	328,958
	70	348,557	354,369	348,385	340,942	336,658	329,487
	75	345,908	352,951	347,789	340,672	336,742	329,695
	80	341,972	349,654	346,927	340,089	335,633	330,484
	85	338,984	347,258	346,458	339,684	335,249	330,786
	90	336,719	344,458	345,968	339,254	334,885	329,786
	95	334,527	341,87	343,715	338,53	334,408	328,239
	100	331,92	339,461	342,852	337,546	333,985	327,758
	105	330,284	337,672	340,912	336,875	333,603	326,751
	110	329,208	335,812	339,846	335,766	332,361	325,872
	115	328,058	333,775	338,544	334,693	331,365	324,985
	120	327,868	332,76	337,715	333,522	330,245	323,853
	125	326,112	331,853	336,166	332,754	329,732	322,908
	130	324,527	330,274	335,048	331,976	328,965	321,878
	135	323,524	328,361	333,458	331,025	327,376	320,862
	140	322,33	327,075	332,52	330,421	326,247	319,548
	145	321,728	325,652	330,515	329,648	325,75	318,868
	150	321,163	324,284	329,756	328,75	324,447	317,436

Average values of the temperatures

time (s)	brake pad thickness (mm)						ΔT 4:8
	2,00	4,00	8,00	10,00	12,00	16,00	
5	301,49	300,24	299,34	298,04	297,30	296,93	0,90
10	317,62	310,73	305,09	301,23	299,29	297,35	5,65
15	331,26	321,04	311,56	304,46	303,00	299,44	9,48
20	342,52	332,18	318,61	310,32	309,71	302,72	13,57
25	358,84	346,81	326,06	317,97	316,36	308,07	20,74
30	371,96	360,92	333,25	326,23	321,20	313,46	27,67
35	373,02	361,92	341,35	330,45	324,89	317,48	20,57
40	371,72	362,33	344,52	334,74	328,18	321,97	17,81
45	369,00	362,51	346,56	337,93	330,44	324,31	15,95
50	365,15	361,17	348,64	340,49	332,78	326,12	12,53
55	360,65	360,45	349,20	342,67	335,46	327,60	11,26
60	357,62	359,13	350,48	343,53	336,79	328,61	8,65
65	353,98	356,96	350,26	343,83	337,38	329,84	6,70
70	351,37	355,11	349,69	343,30	338,28	330,53	5,42
75	349,20	353,32	349,10	343,07	338,94	330,89	4,22
80	346,16	350,54	348,31	342,77	337,80	331,47	2,23
85	343,18	348,46	347,64	342,11	337,24	331,33	0,82
90	340,51	345,75	346,70	341,80	337,13	330,55	-0,95
95	338,28	343,82	345,51	341,05	336,49	329,50	-1,69
100	336,89	341,67	344,27	339,96	335,84	328,77	-2,60
105	334,95	339,58	342,81	338,93	334,78	327,06	-3,23
110	333,95	338,18	341,57	338,04	333,58	325,95	-3,39
115	332,73	336,50	340,12	337,09	332,61	324,77	-3,62
120	331,17	335,37	339,17	336,50	331,75	323,67	-3,79
125	329,78	333,97	337,86	335,47	331,14	322,51	-3,89
130	328,38	332,26	336,17	334,27	329,38	321,32	-3,91
135	327,21	330,61	334,66	333,31	328,29	320,30	-4,06
140	325,96	329,35	333,43	332,29	327,41	319,06	-4,08
145	324,97	327,94	332,22	331,64	326,89	318,15	-4,29
150	323,91	326,75	331,09	330,65	326,06	316,94	-4,35

Temperature evolution through the time

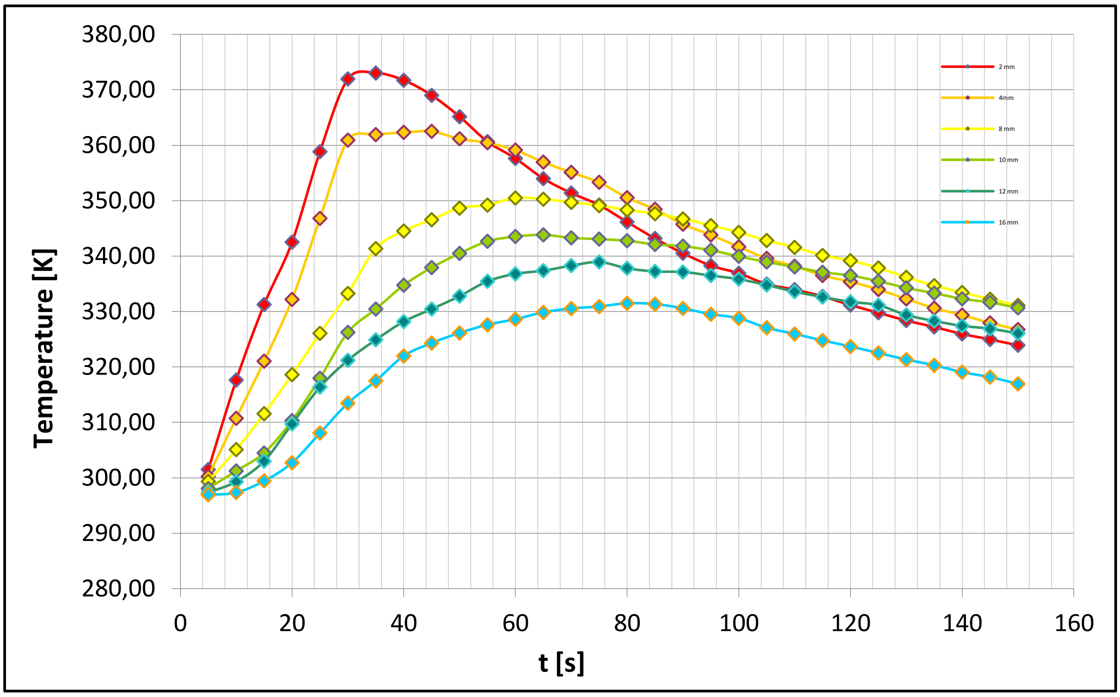

Temperature profile in the brake pad

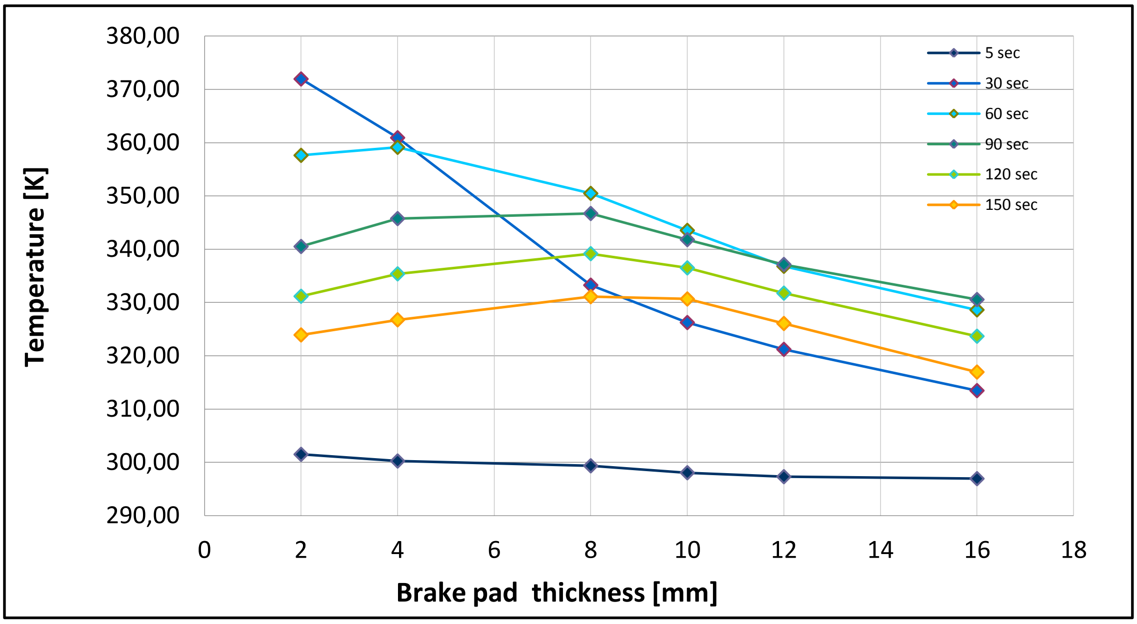

Temperature gadient between 4 and 8 mm

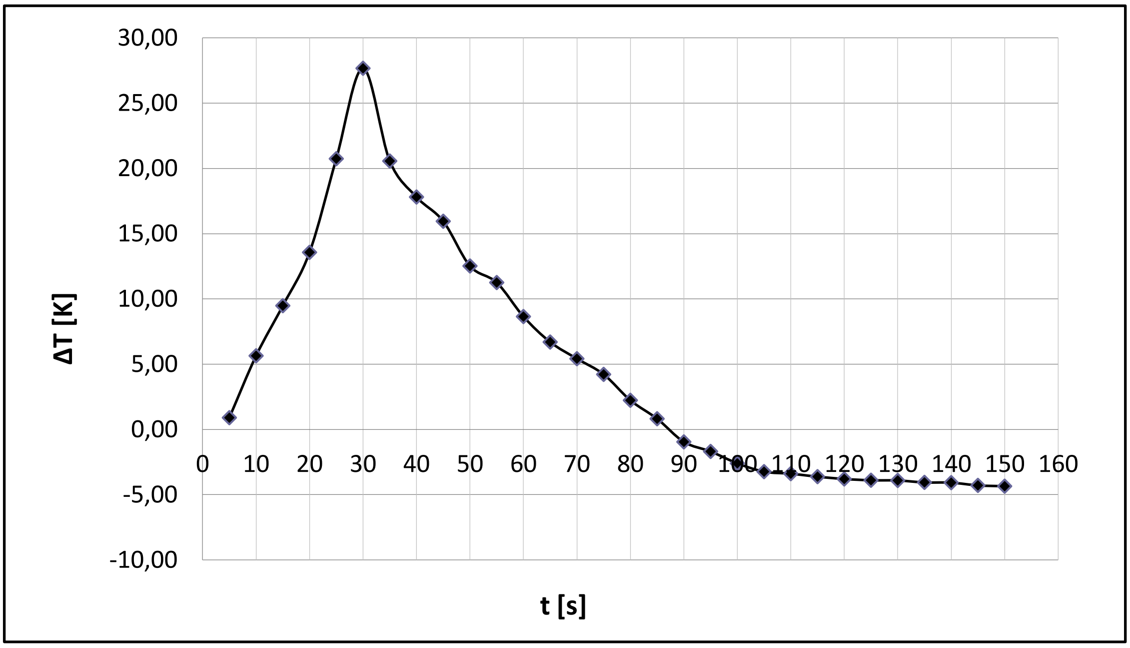

Appendix 8.8 Open circuit voltage after an emergency brake from 30km/h

Results obtained during the four experiments

		Voltage (v)				
		exp 1	exp 2	exp 3	exp 4	average
time (s)	0	-0,00025	0,00018	0,00035	-0,00036	-0,00002
	1	0,00046	0,00386	0,00105	0,00030	0,00142
	2	0,00147	0,00456	0,00219	0,00258	0,00270
	3	0,00456	0,00612	0,00427	0,00510	0,00501
	4	0,00675	0,00676	0,00562	0,00661	0,00643
	5	0,00883	0,00857	0,00867	0,00984	0,00898
	6	0,01076	0,01105	0,01158	0,01134	0,01118
	7	0,01281	0,01305	0,01281	0,01317	0,01296
	8	0,01418	0,01394	0,01284	0,01384	0,01370
	9	0,01160	0,01366	0,01237	0,01160	0,01231
	10	0,01061	0,01279	0,00984	0,00970	0,01073
	11	0,00991	0,01146	0,00928	0,00898	0,00991
	12	0,00878	0,01040	0,00868	0,00857	0,00911
	13	0,00812	0,00906	0,00779	0,00768	0,00816
	14	0,00716	0,00773	0,00708	0,00700	0,00724
	15	0,00654	0,00660	0,00624	0,00586	0,00631
	16	0,00612	0,00603	0,00551	0,00551	0,00579
	17	0,00523	0,00530	0,00514	0,00494	0,00515
	18	0,00463	0,00440	0,00461	0,00358	0,00430
	19	0,00324	0,00301	0,00259	0,00273	0,00289
	20	0,00254	0,00145	0,00166	0,00134	0,00175

Open circuit voltage production through the time

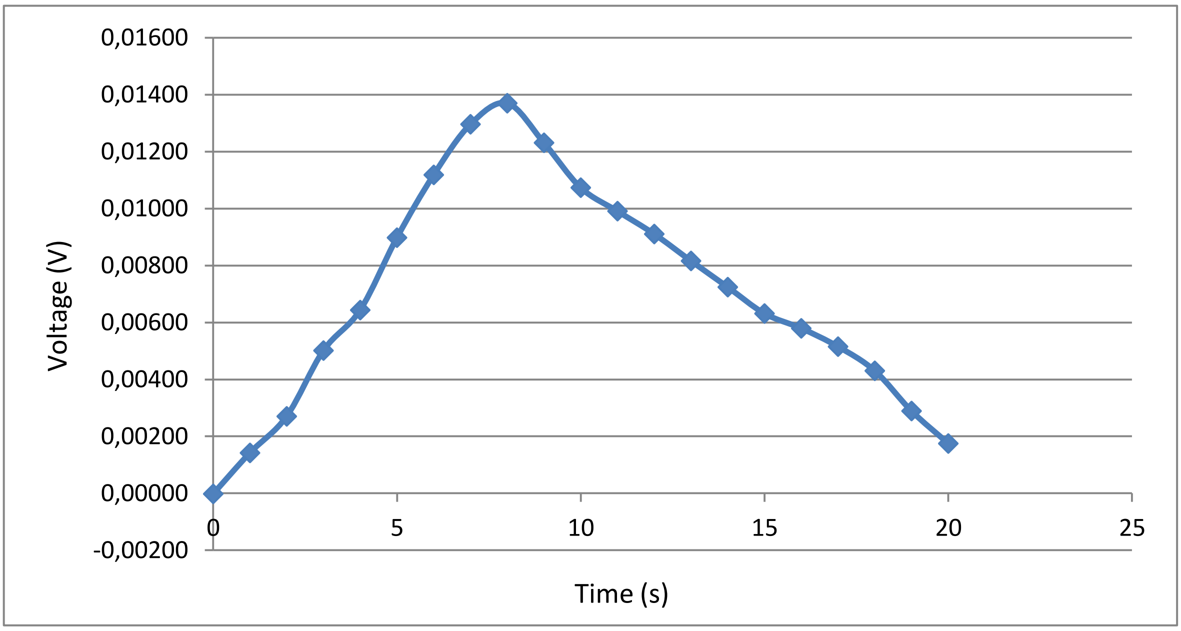

Appendix 8.9 Open circuit voltage after an emergency brake from 50km/h

Results obtained during the four experiments

		Voltage (v)				
		exp 1	exp 2	exp 3	exp 4	average
time (s)	0	-0,00068	0,00026	-0,00018	0,00013	-0,00012
	1	0,00077	0,00108	0,00048	0,00078	0,00078
	2	0,00247	0,00301	0,00222	0,00273	0,00261
	3	0,00509	0,00432	0,00541	0,00487	0,00492
	4	0,00768	0,00831	0,00812	0,00877	0,00822
	5	0,01190	0,01231	0,01157	0,01334	0,01228
	6	0,01385	0,01655	0,01509	0,01572	0,01530
	7	0,01590	0,01682	0,01756	0,01823	0,01712
	8	0,01624	0,01685	0,01575	0,01582	0,01616
	9	0,01260	0,01469	0,01498	0,01345	0,01393
	10	0,01240	0,01176	0,01279	0,01219	0,01228
	11	0,00998	0,00997	0,01208	0,01134	0,01084
	12	0,00906	0,00878	0,01101	0,00984	0,00967
	13	0,00803	0,00763	0,01024	0,00906	0,00874
	14	0,00700	0,00660	0,00875	0,00768	0,00751
	15	0,00664	0,00626	0,00820	0,00675	0,00696
	16	0,00634	0,00606	0,00630	0,00624	0,00623
	17	0,00557	0,00531	0,00550	0,00579	0,00554
	18	0,00411	0,00437	0,00458	0,00532	0,00459
	19	0,00316	0,00407	0,00358	0,00273	0,00338
	20	0,00184	0,00276	0,00287	0,00186	0,00234

Open circuit voltage production through the time

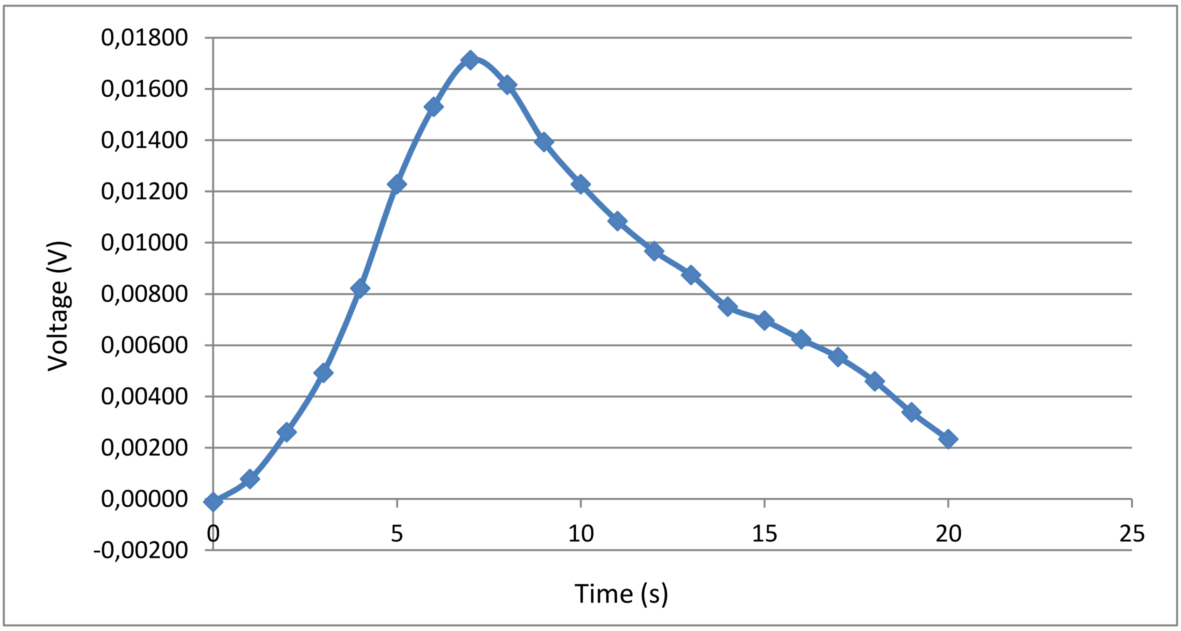

Appendix 8.10 Open circuit voltage after an emergency brake from 70km/h

Results obtained during the four experiments

time (s)	Voltage (v) exp 1	exp 2	exp 3	exp 4	average
0	-0,00054	-0,00016	0,00173	-0,00074	0,00007
1	0,00078	0,00042	0,00282	0,00101	0,00126
2	0,00353	0,00250	0,00565	0,00428	0,00399
3	0,00684	0,00625	0,00935	0,00723	0,00742
4	0,01180	0,01005	0,01204	0,00984	0,01093
5	0,01499	0,01375	0,01600	0,01293	0,01442
6	0,01900	0,01809	0,01782	0,01745	0,01809
7	0,02108	0,02146	0,02176	0,02074	0,02126
8	0,02036	0,02057	0,02007	0,01830	0,01982
9	0,01675	0,01729	0,01860	0,01653	0,01729
10	0,01485	0,01533	0,01588	0,01393	0,01500
11	0,01381	0,01355	0,01392	0,01289	0,01354
12	0,01197	0,01199	0,01281	0,01250	0,01232
13	0,01103	0,01128	0,01120	0,01162	0,01128
14	0,01047	0,00967	0,00990	0,00972	0,00994
15	0,00857	0,00844	0,00857	0,00888	0,00862
16	0,00737	0,00708	0,00676	0,00722	0,00711
17	0,00619	0,00578	0,00613	0,00601	0,00603
18	0,00512	0,00494	0,00503	0,00486	0,00499
19	0,00419	0,00400	0,00406	0,00358	0,00396
20	0,00287	0,00312	0,00244	0,00271	0,00279

Open circuit voltage production through the time

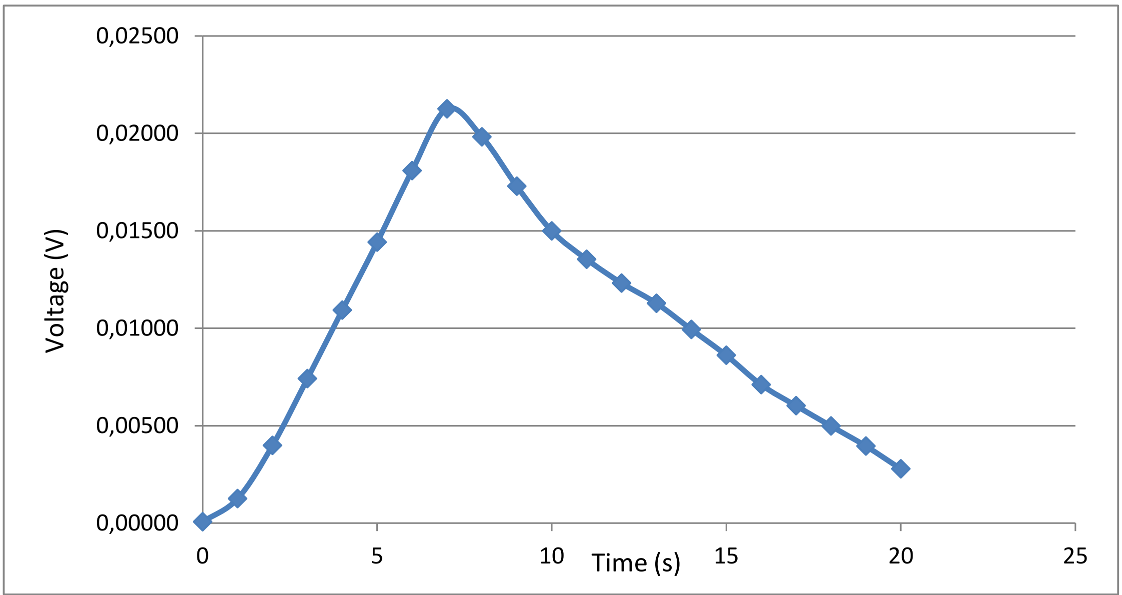

Appendix 8.11 Open circuit voltage during a constant downhill braking

Results obtained during the four experiments

		Voltage (v)				
		exp 1	exp 2	exp 3	exp 4	average
time (s)	0	0,00960	0,00606	0,01201	0,00342	0,00777
	5	0,06246	0,04494	0,05216	0,03670	0,04906
	10	0,12418	0,11387	0,12418	0,10975	0,11799
	15	0,20650	0,18589	0,20650	0,19207	0,19774
	20	0,25802	0,25802	0,26832	0,25183	0,25905
	25	0,31984	0,30953	0,33014	0,31468	0,31855
	30	0,37168	0,38199	0,37689	0,36962	0,37504
	35	0,34042	0,33196	0,34072	0,30526	0,32959
	40	0,29984	0,29014	0,30180	0,29065	0,29561
	45	0,26920	0,26085	0,26951	0,25920	0,26469
	50	0,23923	0,23893	0,23095	0,22408	0,23330
	55	0,21862	0,21832	0,21862	0,20450	0,21502
	60	0,18037	0,17673	0,18319	0,18189	0,18055
	65	0,15619	0,15890	0,14886	0,15001	0,15349
	70	0,12671	0,13036	0,12170	0,12005	0,12471
	75	0,10182	0,11621	0,10213	0,10873	0,10722
	80	0,08757	0,08485	0,08877	0,08939	0,08765
	85	0,05633	0,04664	0,05694	0,06015	0,05502
	90	0,01805	0,02135	0,01787	0,02870	0,02149

Open circuit voltage production through the time

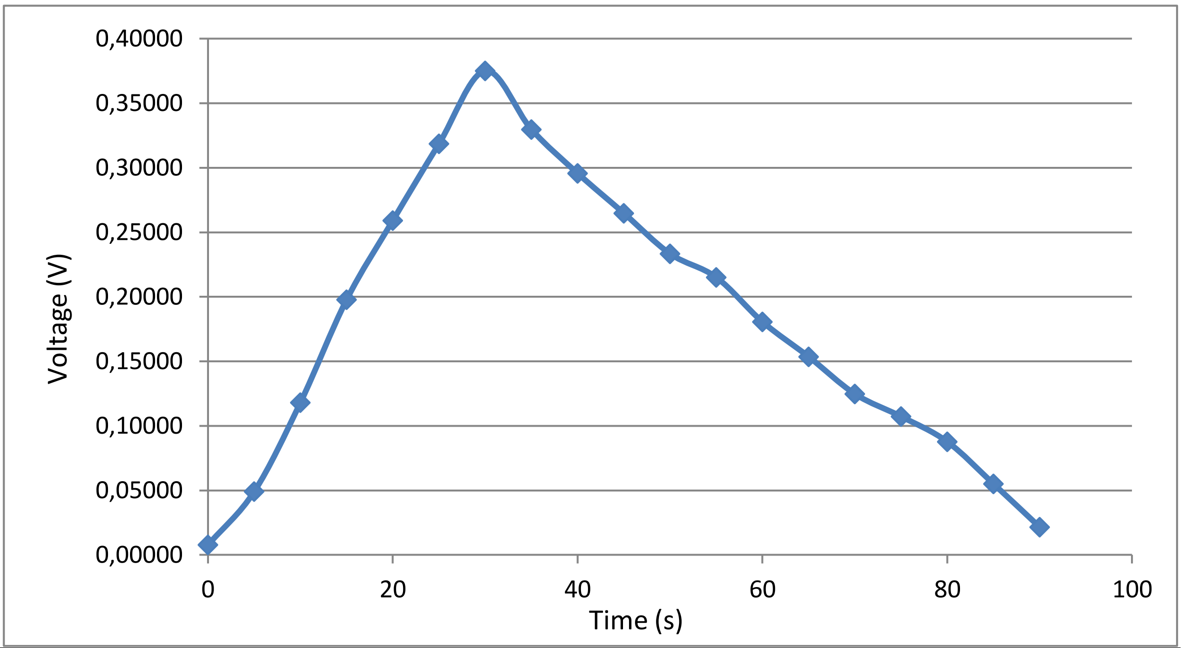

Appendix 8.12 Open circuit voltage during an urban drving cycle

Results obtained during the 2 experiments

		Voltage (V)		
		exp 1	exp 2	average
Time (s)	0	0,00043	0,00064	0,00054
	5	0,00067	0,00054	0,00060
	10	0,00081	0,00024	0,00053
	15	0,00066	0,00010	0,00038
	20	0,00082	0,00028	0,00055
	25	0,00098	0,00004	0,00051
	30	0,00183	0,00195	0,00189
	35	0,00865	0,00990	0,00927
	40	0,01688	0,01565	0,01626
	45	0,02061	0,02058	0,02059
	50	0,02531	0,02728	0,02629
	55	0,03043	0,02898	0,02970
	60	0,02839	0,02579	0,02709
	65	0,02569	0,02492	0,02531
	70	0,02257	0,02330	0,02294
	75	0,02023	0,02120	0,02072
	80	0,03884	0,03834	0,03859
	85	0,04032	0,04535	0,04283
	90	0,05733	0,05527	0,05630
	95	0,06283	0,06293	0,06288
	100	0,07840	0,07737	0,07789
	105	0,08763	0,08753	0,08758
	110	0,09853	0,09225	0,09539
	115	0,09338	0,09016	0,09177
	120	0,09176	0,08723	0,08949
	125	0,08947	0,08543	0,08745
	130	0,08504	0,08237	0,08371
	135	0,08361	0,07858	0,08110
	140	0,07992	0,07468	0,07730
	145	0,07623	0,07104	0,07363
	150	0,07387	0,06862	0,07125
	155	0,07116	0,06613	0,06864
	160	0,08568	0,08065	0,08316
	165	0,10235	0,09732	0,09984
	170	0,11767	0,11561	0,11664
	175	0,13058	0,12928	0,12993
	180	0,14384	0,14354	0,14369
	185	0,16043	0,16012	0,16028
	190	0,17336	0,17518	0,17427
	195	0,18165	0,18965	0,18565
	200	0,17938	0,17928	0,17933
	205	0,17468	0,17468	0,17468

time (s)	210	0,16953	0,16953	0,16953
	215	0,16501	0,16501	0,16501
	220	0,16198	0,16028	0,16113
	225	0,15529	0,15616	0,15573
	230	0,14962	0,15165	0,15063
	235	0,15526	0,15488	0,15507
	240	0,16059	0,15847	0,15953
	245	0,16526	0,16223	0,16374
	250	0,16904	0,16616	0,16760
	255	0,17613	0,17017	0,17315
	260	0,17420	0,16626	0,17023
	265	0,16957	0,16060	0,16508
	270	0,16324	0,15936	0,16130
	275	0,15985	0,15488	0,15736
	280	0,15448	0,15251	0,15349
	285	0,15941	0,15744	0,15842
	290	0,16496	0,16268	0,16382
	295	0,17136	0,16830	0,16983
	300	0,17798	0,17486	0,17642
	305	0,18287	0,17990	0,18139
	310	0,18023	0,17526	0,17774
	315	0,17557	0,17169	0,17363
	320	0,17185	0,16782	0,16983
	325	0,16648	0,16242	0,16445
	330	0,16176	0,15791	0,15983
	335	0,15739	0,15240	0,15489
	340	0,15269	0,14960	0,15114
	345	0,14856	0,14515	0,14686
	350	0,14330	0,14135	0,14233
	355	0,13995	0,13793	0,13894
	360	0,14622	0,14519	0,14571
	365	0,15144	0,15300	0,15222
	370	0,15813	0,16023	0,15918
	375	0,16344	0,16732	0,16538
	380	0,16680	0,17249	0,16964
	385	0,17380	0,17936	0,17658
	390	0,17783	0,18410	0,18096
	395	0,18274	0,18961	0,18617
	400	0,18883	0,19328	0,19105
	405	0,19201	0,19832	0,19517
	410	0,18568	0,19258	0,18913
	415	0,18053	0,17754	0,17904
	420	0,17671	0,17230	0,17451
	425	0,17116	0,16675	0,16896
	430	0,16680	0,16261	0,16470
	435	0,16241	0,15470	0,15855
	440	0,16462	0,15807	0,16134
	445	0,16831	0,16110	0,16470
	450	0,17139	0,16497	0,16818
	455	0,17461	0,16845	0,17153

time (s)	460	0,17738	0,17200	0,17469
	465	0,17168	0,16806	0,16987
	470	0,16753	0,16496	0,16624
	475	0,16124	0,16063	0,16094
	480	0,16353	0,16343	0,16348
	485	0,16720	0,16661	0,16690
	490	0,16927	0,16968	0,16948
	495	0,17281	0,17228	0,17255
	500	0,17562	0,17475	0,17518
	505	0,17833	0,17759	0,17796
	510	0,17255	0,17201	0,17228
	515	0,16752	0,16774	0,16763
	520	0,16148	0,16370	0,16259
	525	0,15812	0,15879	0,15846
	530	0,15562	0,15407	0,15485
	535	0,15233	0,15159	0,15196
	540	0,14955	0,14701	0,14828
	545	0,14652	0,14374	0,14513
	550	0,14248	0,14070	0,14159
	555	0,13912	0,13688	0,13800
	560	0,14652	0,14174	0,14413
	565	0,15148	0,14770	0,14959
	570	0,15512	0,15379	0,15446
	575	0,15996	0,16033	0,16015
	580	0,16571	0,16745	0,16658
	585	0,17173	0,17215	0,17194
	590	0,17758	0,17705	0,17732
	595	0,18144	0,18166	0,18155
	600	0,18556	0,18523	0,18539
	605	0,18960	0,18717	0,18838
	610	0,18471	0,18103	0,18287
	615	0,18082	0,17679	0,17880
	620	0,17507	0,17131	0,17319
	625	0,16803	0,16648	0,16725
	630	0,16283	0,16061	0,16172
	635	0,16254	0,16266	0,16260
	640	0,16573	0,16608	0,16591
	645	0,16794	0,16923	0,16859
	650	0,17002	0,17179	0,17091
	655	0,17300	0,17312	0,17306
	660	0,16876	0,16634	0,16755
	665	0,16255	0,16154	0,16204
	670	0,15700	0,15688	0,15694
	675	0,15280	0,15276	0,15278
	680	0,15462	0,15155	0,15308
	685	0,15726	0,15639	0,15682
	690	0,16048	0,16191	0,16119
	695	0,16305	0,16473	0,16389
	700	0,16819	0,16909	0,16864
	705	0,16919	0,17112	0,17016

time (s)	710	0,16304	0,16791	0,16548
	715	0,15961	0,16302	0,16132
	720	0,15540	0,15784	0,15662
	725	0,15141	0,15246	0,15193
	730	0,14716	0,14879	0,14798
	735	0,14302	0,14538	0,14420
	740	0,13913	0,14012	0,13962
	745	0,13625	0,13486	0,13555
	750	0,13297	0,12913	0,13105
	755	0,12876	0,12407	0,12642
	760	0,13501	0,12810	0,13156
	765	0,14163	0,13579	0,13871
	770	0,14725	0,14922	0,14824
	775	0,15276	0,15471	0,15373
	780	0,15692	0,15829	0,15761
	785	0,16191	0,16352	0,16271
	790	0,16543	0,16671	0,16607
	795	0,16906	0,17057	0,16982
	800	0,17358	0,17491	0,17424
	805	0,17652	0,17706	0,17679
	810	0,17067	0,17189	0,17128
	815	0,16528	0,16615	0,16571
	820	0,16078	0,16170	0,16124
	825	0,15740	0,15585	0,15662
	830	0,15201	0,15205	0,15203
	835	0,14872	0,14863	0,14868
	840	0,14483	0,14354	0,14419
	845	0,14064	0,13875	0,13969
	850	0,13698	0,13591	0,13645
	855	0,13379	0,13173	0,13276
	860	0,12902	0,12875	0,12889
	865	0,12564	0,12591	0,12577
	870	0,12032	0,12173	0,12102
	875	0,11682	0,11711	0,11696
	880	0,11186	0,11292	0,11239
	885	0,10658	0,10820	0,10739
	890	0,10284	0,10366	0,10325
	895	0,09835	0,09934	0,09884
	900	0,09488	0,09525	0,09507

Open circuit voltage production through the time

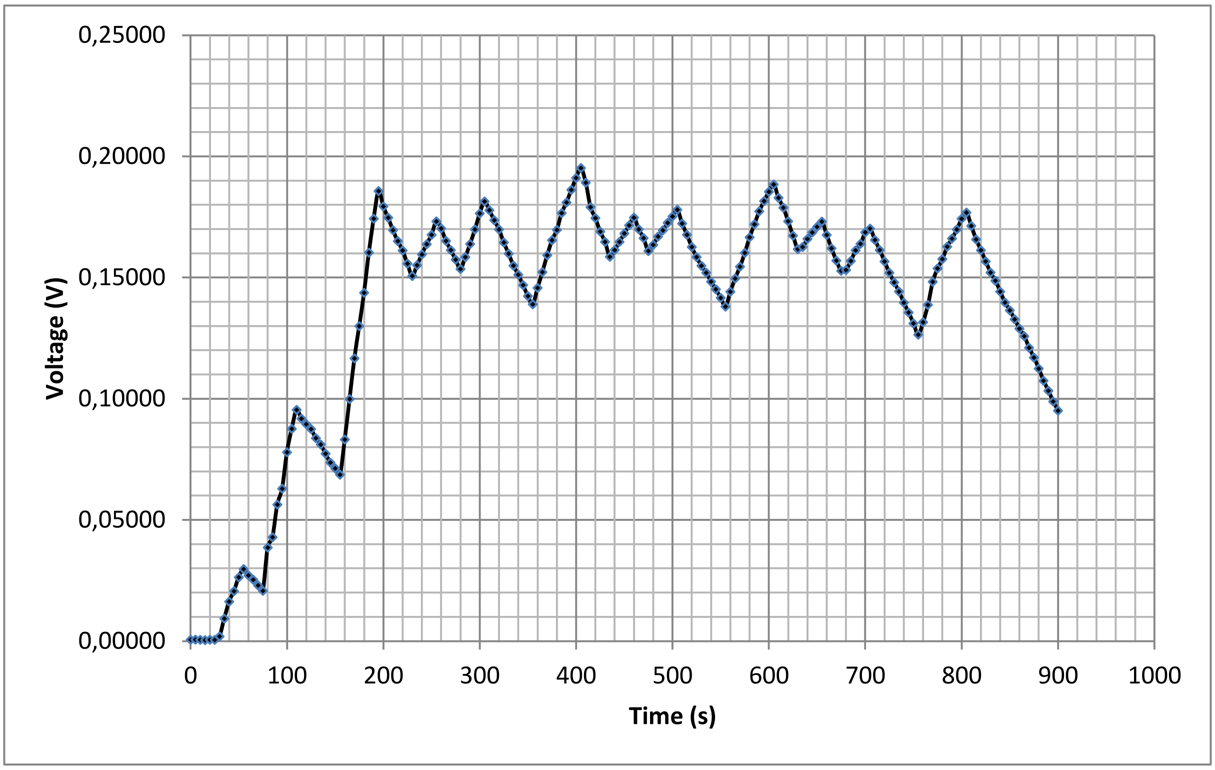

Appendix 8.13 Power generation experiment

TEG resistance in fuction of the temperature

tpt (K)	Resistance (R)
297	1,25
300	5,2
310	18,43
320	39,53
330	60,76
340	82,59
350	105,4
360	123,58
370	142,36
380	163,24
390	181,15
400	197,2

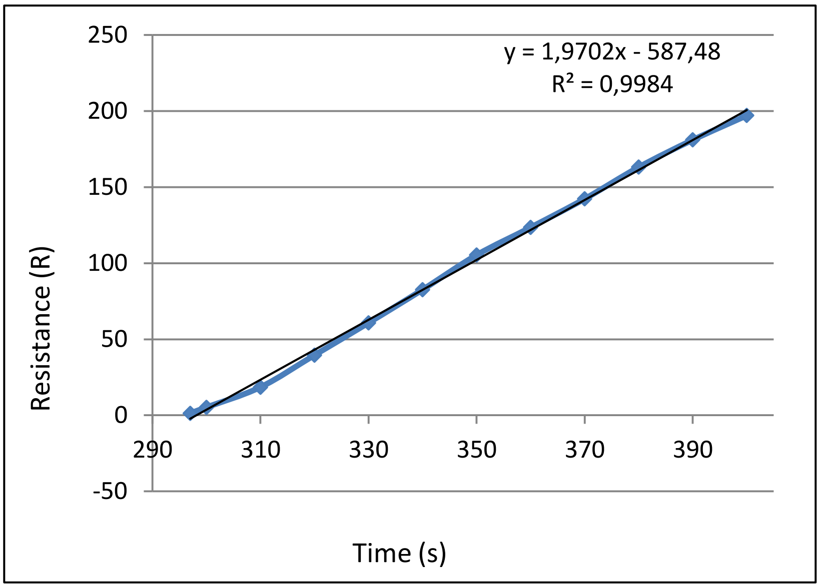

Temperature, resistance voltage and power through the time

time (s)	tpt (K)	Resistance (R)	Voltage (V)	Power (W)
5	302,213	7,87961	0,018414359	4,303E-05
10	318,862	40,67814	0,062595615	9,632E-05
15	330,139	62,89383	0,100457468	1,605E-04
20	341,034	84,35698	0,13632913	2,203E-04
25	359,552	120,83744	0,185157847	2,837E-04
30	372,415	146,17755	0,226304814	3,504E-04
35	373,746	148,79962	0,24819362	4,140E-04
40	372,884	147,10148	0,238738625	3,875E-04
45	371,99	145,3403	0,222650593	3,411E-04
50	369,331	140,10207	0,197252308	2,777E-04
55	365,407	132,37179	0,167437273	2,118E-04
60	362,714	127,06658	0,14516032	1,658E-04
65	359,034	119,81698	0,125557616	1,316E-04
70	356,203	114,23991	0,100432328	8,829E-05
75	354,651	111,18247	0,087037999	6,814E-05
80	350,012	102,04364	0,060923591	3,637E-05
85	347,768	97,62296	0,045891032	2,157E-05
90	343,289	88,79933	0,028560831	9,186E-06

Pmoy	1,837E-04
E tot	1,654E-02

Voltage through the time

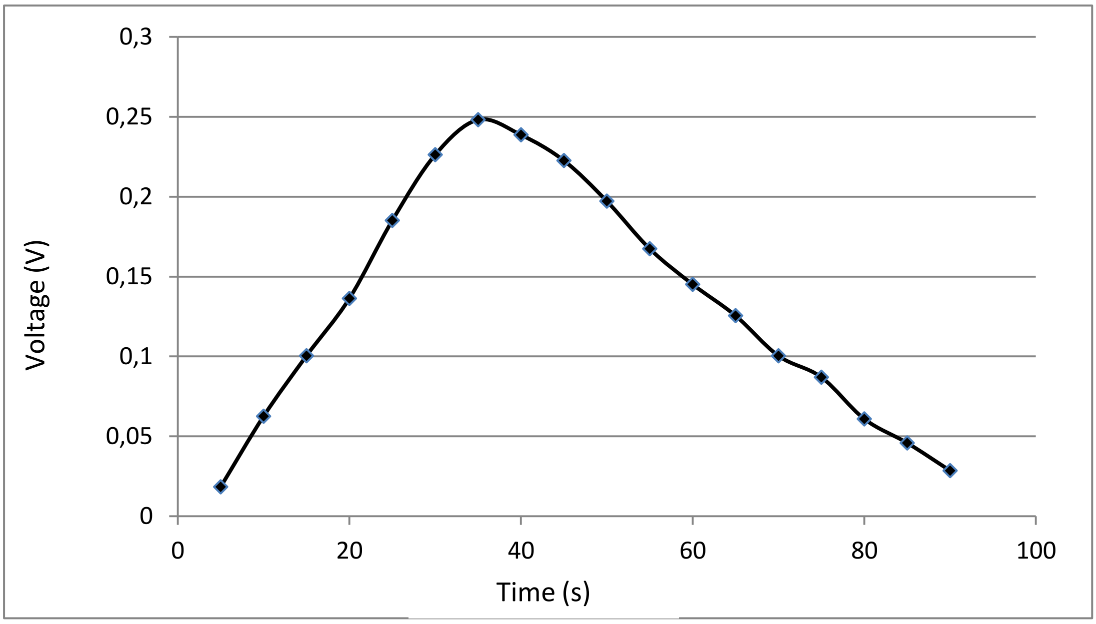

Power generation through the time